AD_____

Award Number: DAMD17-01-1-0145

TITLE: Genetic and Functional Studies of Genes that Regulate DNA-Damage-Induced Cell Death

PRINCIPAL INVESTIGATOR: Zhou Songyang, Ph.D.

CONTRACTING ORGANIZATION: Baylor College of Medicine
Houston, TX 77030

REPORT DATE: November 2005

TYPE OF REPORT: Final

PREPARED FOR: U.S. Army Medical Research and Materiel Command
Fort Detrick, Maryland 21702-5012

REPORT DOCUMENTATION PAGE

Form Approved
OMB No. 0704-0188

1. REPORT DATE *(DD-MM-YYYY)*	2. REPORT TYPE	3. DATES COVERED *(From - To)*
01-11-2005	Final	1 May 2001 - 31 Oct 2005

4. TITLE AND SUBTITLE
Genetic and Functional Studies of Genes that Regulate DNA-Damage-Induced Cell Death

5a. CONTRACT NUMBER

5b. GRANT NUMBER
DAMD17-01-1-0145

5c. PROGRAM ELEMENT NUMBER

6. AUTHOR(S)
Zhou Songyang, Ph.D.

E-mail: songyang@bcm.tmc.edu

5d. PROJECT NUMBER

5e. TASK NUMBER

5f. WORK UNIT NUMBER

7. PERFORMING ORGANIZATION NAME(S) AND ADDRESS(ES)
Baylor College of Medicine
Houston, TX 77030

8. PERFORMING ORGANIZATION REPORT NUMBER

9. SPONSORING / MONITORING AGENCY NAME(S) AND ADDRESS(ES)
U.S. Army Medical Research and Materiel Command
Fort Detrick, Maryland 21702-5012

10. SPONSOR/MONITOR'S ACRONYM(S)

11. SPONSOR/MONITOR'S REPORT NUMBER(S)

12. DISTRIBUTION / AVAILABILITY STATEMENT
Approved for Public Release; Distribution Unlimited

13. SUPPLEMENTARY NOTES

14. ABSTRACT
Studies have shown that apoptosis and survival pathways in response to DNA damage play a critical role in breast cancer development and progression. 90% of breast cancer cases are sporadic where mutations of BRCA1/2 have not been detected. Other breast cancer genes must exist. Our group has approached the issue in two ways, a genomic and a proteomic approach. We have established and utilized a novel retrovirus-based genetic screen system to search for genes that would confer resistance to DNA dmage induced apoptosis. Multiple clones have been isolated from this genetic screen. Among the genes identified are both novel and known proteins that may be important in DNA-damage responses. To further elucidate the pathways mediated by BARD1, we looked for factors interacting with BARD1 using mass spec sequencing. Several factors have emerged from this study and are being examined. The information obtained from our studies should prove useful for developing new and effective screening strategies, drug targets, and treatment for breast cancer.

15. SUBJECT TERMS
oncogenes, tumor suppressor, genome-wide, genetic screen, retrovirus, apoptosis, cell survival, BRCA1, BARD1, DNA damage, cancer

16. SECURITY CLASSIFICATION OF:			17. LIMITATION OF ABSTRACT	18. NUMBER OF PAGES	19a. NAME OF RESPONSIBLE PERSON
					USAMRMC
a. REPORT	b. ABSTRACT	c. THIS PAGE			19b. TELEPHONE NUMBER *(include area code)*
U	U	U	UU	29	

Table of Contents

Introduction

Understanding the molecular and cellular mechanisms that trigger breast cancer is essential to the prevention and treatment of this disease. The initiation and progression of breast cancer is likely the result of dysregulation of both oncogenes and tumor suppressor genes (1, 2). Mutations of these genes can cause defects in cellular survival and proliferation, genomic integrity, and sensitivity to DNA damage. However, few genes that regulate DNA damage induced cell death are known to date, and even less is known as to how they interconnect with the apoptosis and survival pathways. We have proposed to establish a genetic system to screen for genes that regulate survival in cultured cells through high-efficiency mutagenesis using Enhanced Retroviral Mutagens (ERM) (3). Due to the random nature of retroviral integration, endogenous genes involved in cell survival signaling cascades may be activated or inactivated by ERM. The targeted gene loci are marked by retroviral integration thereby allowing quick isolation of the candidate genes. The overall objective of this proposal is to identify and study genes that allow the survival of normal and cancerous breast cells. The physiological roles of these genes and their interactions with known signaling pathways will be investigated. Genetic screens will be performed to search for survival genes in response to DNA damage. And the function and signaling mechanisms of BARD1 in breast cancer cell survival will also be examined. The proposed studies should help in our understanding of the molecular basis underlying cell survival signaling and breast cancer as well as provide new therapeutic targets for the cure of this disease.

Body

(1) For Task 1, we proposed to isolate mammalian genes involved in breast cancer cell survival. This will be achieved by establishing Enhanced Retrovirus Mutagen (ERM)-mediated genetic screen and analyzing isolated clones, establishing secondary screens using human breast epithelial cells to confirm the role the cloned genes in DNA-damage-induced apoptosis, and identifying the candidate genes targeted by ERM.

In previous reports, we described the development and employment of our retrovirus-based genetic screen system ERM (3) to ientify genes that mediate DNA-damage induced apoptosis. We optimized the ERM approach, by engineering different tag sequences (such as epitope and signaling tags). Table 1 lists some of the vectors generated for the ERM screen. In addition, all ERM vectors contain the tetrocycline responsive promoter.

Tags	Name	Advantage
Epitope tag	HA, FLAG, AU3	Detection of fusion gene products
Signaling tag	Myristylation signal (Myr)	Membrane targeting to ↑ efficiency
Protein tag	GFP	Visualization of targeted gene products in live cells

Table 1. List of vectors for ERM-mediated genetic screen.

Primary and secondary screens were then carried out. The strategy was first used to investigate DNA-damage induced cell death in a cytokine-dependent cell line. The retroviral

mutagen constructs were transfected into a retroviral packaging cell line and the viruses were harvested 48 hours post transfection (Figure 1). These viruses were then used to infect the cytokine-dependent cell line 32D cells at MOI <=1 (3). These infected cells were first cultured in flasks for 3 days in the presence of the DNA-damage inducing drug cisplatin (CDDP) at a concentration of 50mM. Under this condition, >95% of the 32D cells underwent apoptosis (Figure 2). Subsequently, the cells were washed to eliminate CDDP, and plated in 6 x 96-well plates at approximately 1,000 cells per well. Multiple clones have been isolated from this genetic screen. In Table 2, we listed a number of genes that we have identified to date. In addition, we have carried out secondary screens in human breast epithelial cells to confirm the role of the cloned genes in DNA-damage-induced apoptosis. We are currently preparing a manuscript that describes the data from these experiments.

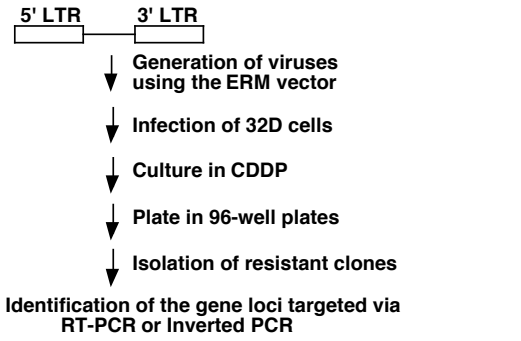

Figure 1. Flow chart for ERM-mediated genetic screen

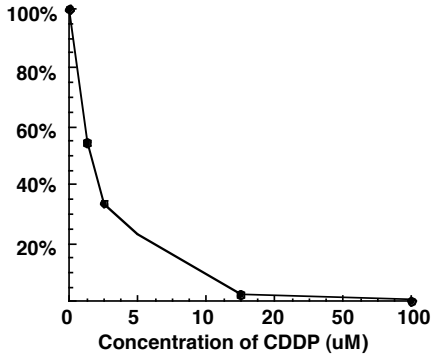

Figure 2 Survival of 32D cells in different concentrations of CDDP

Genes	Possible function
novel	Conserved through evolution. Binds to RAD50
NESH	Homologue of Abi-1. SH3 domain containing protein
novel	Unknown function
Lyn	Tyrosine kinase. Involved in DNA-damage response (4-7).

Table 2. Sample list of identified genes.

(2) For Task 2, we have proposed to biochemically characterize breast cancer genes including how BARD1 may be involved in breast cancer cell survival. BARD1 was cloned originally as an interactor of BRCA1 and has been implicated as a critical factor in BRCA1 tumor suppression (8). Missense, point mutation and loss-of-function mutations of BARD1 have been found in breast cancers (9).

BARD1 contains an N-terminal RING finger, ankyrin repeats, and C-terminal BRCT domains (Figure 3). To test the role of BARD1 in apoptosis, we compared the survival rate of cells expressing wildtype BARD1 and mutant BARD1 (□53) in which RING finger was

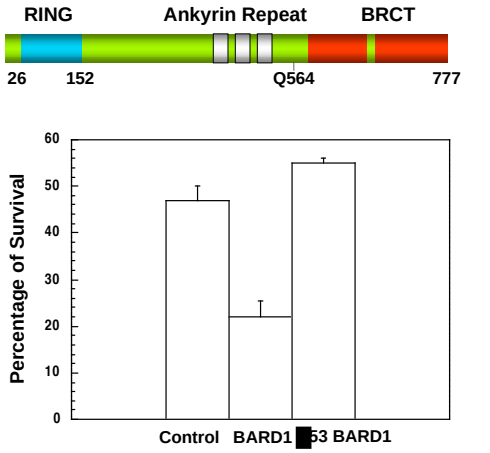

Figure 3. BARD1 promotes IL-3 deprivation induced apoptosis. 32D Cell survival was compared 17 hrs after IL-3 withdrawal.

deleted following IL-3 depletion. As shown in Figure 3, expression of full-length BARD1 increased apoptosis of 32D cells, whereas 53 BARD1 cells no longer promoted cell death (in fact survived better than control cells). These data suggest that the RING finger may be important for BARD1 apoptosis induction activity. Our preliminary results also suggest that BARD1 may modulate cell survival in response to DNA damage. However, the mechanism of how BARD1 modulates apoptosis remains to be elucidated.

One way to dissect the function of BARD1 is through analysis of the factors that may interact with BARD1. To accomplish this, we optimized a proteomic approach (Figure 4). Briefly, large amount of human HeLa cells were grown and harvested. Nuclear extracts were made from these cells and then immunoprecipitated in large-scale with an anti-BARD1 antibody. The immunoprecipitates were subsequently resolved by SDS-PAGE, and visualized by Coomassie Blue Staining. Desired bands were then excised from the gels, digested, and sequenced via Mass Spectrometry.

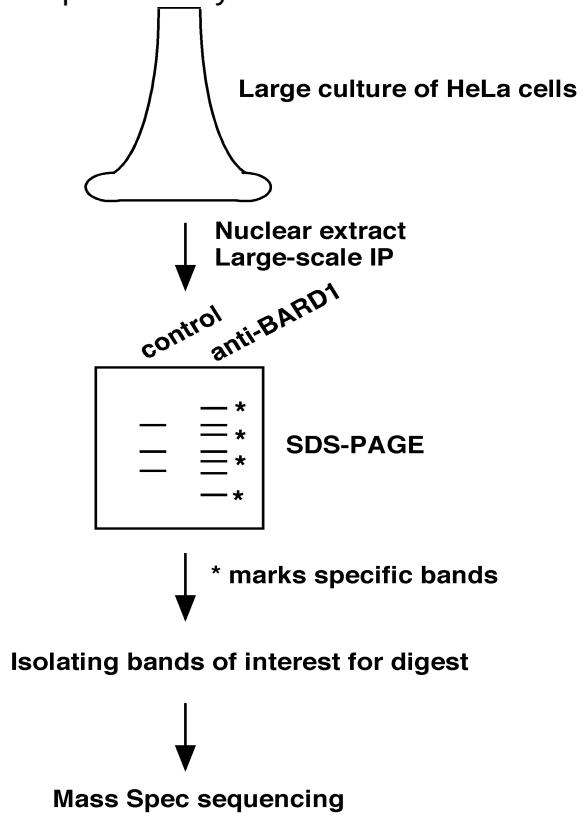

Figure 4. Flowchart of large-scale IP approach.

Through this proteomic method, we identified a number of factors known to interact with BARD1. Factors that are known to interact with BARD1 were identified (e.g., BRCA1 and CstF50). In addition, we also identified three novel factors (Table 3). To further characterize these interactions, we have obtained cDNAs of all these factors. These cDNAs are in the Gateway vector system. The Gateway system allows for quick and easy shuffling of sequences into a variety of destination vectors, thereby greatly facilitating our mutagenesis and expression/interaction studies.

Genes	Known Function
CPSF-160	multisubunit cleavage and polyadenylation specificity factor (11,12).
CPSF-73	multisubunit cleavage and polyadenylation specificity factor (11, 12).
Symplekin	Complexes with BARD1 associated proteins (13).

Table 3. Some factors known to interact with BARD1.

As mentioned above, BARD1 is a BRCT-domain containing protein. In fact, several of the genes involved in breast cancer contain the BRCT domains (which were originally identified in BRCA1). BRCT domains had been known to mediate protein-protein interaction domains. Because protein phosphorylation plays a major role in regulating DNA-damage induced responses, we went on to probe whether BRCT domains could mediate phosphorylation-dependent interactions. To achieve this, we utilized oriented peptide libraries to map the sequence motifs recognized by the BRCT domains. Through these studies, we demonstrated that these domains can indeed mediate phosphorylation-dependent interactions. Furthermore, such interactions are critical for their function (10). More detailed experiments and results can be found in our published manuscript in the Appendix.

BRCT domains can also be found in proteins not yet implicated in breast cancer development. One example is RAP1, a telomere targeted protein that also contains a Myb domain and a coil-coil domain. Mammalian telomeres consist of long stretches of TTAGGG repeats that serve to protect the ends of chromosomes. To date, a multitude of factors (including DNA-damage response factors such as the MRN complex) have been demonstrated to be targeted to telomeres. The resulting protein/telomere complex is thought to help prevent chromosomal ends from being recognized as DNA breaks. The presence of BRCT domains in telomere proteins and the intrinsic connection between DNA damage response pathways and telomere biology suggest a possible role of telomere proteins in DNA damge reponse, checkpoint activation, and cancer.

To probe this connection further, we first examined the specificity of the RAP1 BRCT domain. However, we found no evidence that the RAP1 BRCT domain is capable of mediating phosphorylation-dependent interactions. In the meantime, we also carried out proteomic analysis as was done for isolating the BARD1 complex. We have isolated complexes that associated with RAP1 and a novel telomere targeted protein that was isolated in the lab -- PTOP. We found both DNA damage response factors and other novel regulators to complex with these proteins (14-16) (see Appendix for details). This is consisternt with the finfing that BRCA1 also interacts with DNA damage response factors

and regulates telomere length and protection (17). More studies are underway to elucidate the interaction between the pathways.

Key Research Accomplishments

- Establishment and improvement of the ERM genetic screen approach
- Generation of CDDP resistant 32D cell clones
- Establishment of a system to identify BARD1 associated factors
- Successful identification of a number of novel factors from the genetic screen
- Successful identification of a number of novel factors from the proteomic approach
- Manuscripts:

1. Rodriguez M, Yu X, Chen J, and Songyang Z. (2003) Phosphopeptide binding specificities of BRCT domains. *J Biol Chem.* 278: 52914-8.

2. OConnor MS, Safari A, Liu D, Qin J, and Songyang Z. (2004) The human Rap1 protein complex and modulation of telomere length. *J Biol. Chem*. 279(27):28585-91.

3. Liu D, Safari A, O'Connor MS, Chan DW, Laegeler A, Qin J, Songyang Z. (2004) PTOP interacts with POT1 and regulates POT1 telomeric localization. *Nat. Cell Biol.* 6(7):673-80.

4. Liu D, O'Connor MS, Qin J, Songyang Z. (2004) Telosome, a mammalian telomere-associated complex formed by multiple telomeric proteins. *J Biol. Chem.* 279(49):51338-42.

5. Liu, D., Songyang Z. Identification of DNA-damage induced survival genes using ERM. *Manuscript in preparation*.

- Meeting abstracts:

Genetic Studies of Genes that Regulate DNA-damage-induced Cell Death. Era of Hope 2002 DOD Breast Cancer Research Program Meeting. Orlando, FL. Sept. 27, 2002.

Reportable Outcomes

We have successfully utilized the ERM approach to identify genes that would confer resistance to CDDP induced cell death. Among the genes identified are both novel and known factors. We have also used a proteomic approach to identify factors in the BARD1 complex.

1. Publications:

Rodriguez M, Yu X, Chen J, and Songyang Z. (2003) Phosphopeptide binding specificities of BRCT domains. *J Biol Chem.* 278: 52914-8.

OConnor MS, Safari A, Liu D, Qin J, and Songyang Z. (2004) The human Rap1 protein complex and modulation of telomere length. *J Biol. Chem*. 279(27):28585-91.

Liu D, Safari A, O'Connor MS, Chan DW, Laegeler A, Qin J, Songyang Z. (2004) PTOP interacts with POT1 and regulates POT1 telomeric localization. *Nat. Cell Biol.* 6(7):673-80.

Liu D, O'Connor MS, Qin J, Songyang Z. (2004) Telosome, a mammalian telomere-associated complex formed by multiple telomeric proteins. *J Biol. Chem.* 279(49):51338-42.

2. Meeting abstracts:

Genetic Studies of Genes that Regulate DNA-damage-induced Cell Death. Era of Hope 2002 DOD Breast Cancer Research Program Meeting. Orlando, FL. Sept. 27, 2002.

3. Degrees obtained:

Jun Xu, Matthew O'Connor, and Maria Rodriguez were graduate students who were supported by the grant. Jun Xu and Matthew O'Connor have recently graduated from Baylor College of Medicine and received their Ph.D. Maria Rodriguez has demonstrated such productivity and excellence that she was recently awarded an NIH NRSA predoctoral fellowship.

4. Development of cell lines, tissue and serum repositories, and other reagents:

CDDP resistant 32D cell clones
CDDP resistant MCF7 clones
Antibodies against various BARD1 complexed proteins
A collection of ERM vectors for various genetic screens

List of personnel receiving pay

Zhou Songyang
Jun Xu
Matthew O'Connor
Defeng Deng
Xiaoning Peng
Ma Wan
Maria Rodriguez
Amin Safari

Huawei Xin

Conclusions

In summary, we have improved and successfully utilized our genetic screen approach for high efficiency mutagenesis. Multiple clones have been isolated and some of the gene loci targeted by the ERM mutagen have also been identified. Furthermore, we are on our way to elucidate how BARD1 may affect cell survival through its interaction with other factors. The information obtained from our studies should prove especially useful for the development of new and effective screening strategies, drug targets, and treatment for breast cancer.

References

1. Ellisen, L. W., and D. A. Haber. 1998. Hereditary breast cancer. Annu Rev Med 49:425-36.

2. Rahman, N., and M. R. Stratton. 1998. The genetics of breast cancer susceptibility. Annu Rev Genet 32:95-121.

3. Liu, D., Yang, X., Yang, D., Songyang, Z. 2000. Genetic screens in mammalian cells using Enhanced Retroviral Mutagens. Oncogene 19:5964-72.

4. Yoshida K, Weichselbaum R, Kharbanda S, Kufe D. 2000. Role for Lyn tyrosine kinase as a regulator of stress-activated protein kinase activity in response to DNA damage. Mol Cell Biol 20:5370-80.

5. Maruo A, Oishi I, Sada K, Nomi M, Kurosaki T, Minami Y, Yamamura H. 1999 Protein tyrosine kinase Lyn mediates apoptosis induced by topoisomerase II inhibitors in DT40 cells. Int Immunol 11:1371-80.

6. Kharbanda S, Saleem A, Yuan ZM, Kraeft S, Weichselbaum R, Chen LB, Kufe D. 1996. Nuclear signaling induced by ionizing radiation involves colocalization of the activated p56/p53lyn tyrosine kinase with p34cdc2. Cancer Res 56:3617-21.

7. Kharbanda S, Yuan ZM, Taneja N, Weichselbaum R, Kufe D. 1994. p56/p53lyn tyrosine kinase activation in mammalian cells treated with mitomycin C. Oncogene 9:3005-11.

8. Wu, L. C., Z. W. Wang, J. T. Tsan, M. A. Spillman, A. Phung, X. L. Xu, M. C. Yang, L. Y. Hwang, A. M. Bowcock, and R. Baer. 1996. Identification of a RING protein that can interact in vivo with the BRCA1 gene product. Nat Genet 14:430-40.

9. Thai, T. H., F. Du, J. T. Tsan, Y. Jin, A. Phung, M. A. Spillman, H. F. Massa, C. Y. Muller, R. Ashfaq, J. M. Mathis, D. S. Miller, B. J. Trask, R. Baer, and A. M. Bowcock. 1998. Mutations in the BRCA1-associated RING domain (BARD1) gene in primary breast, ovarian and uterine cancers. Hum Mol Genet 7:195-202.

10. Rodriguez M, Yu X, Chen J, and Songyang Z. (2003) Phosphopeptide binding specificities of BRCT domains. *J Biol Chem.* 279:8802-7.

11. Dichtl B, Blank D, Sadowski M, Hubner W, Weiser S, Keller W. 2002. Yhh1p/Cft1p directly links poly(A) site recognition and RNA polymerase II transcription termination. EMBO J 21: 4125-35.

12. Salinas CA, Sinclair DA, O'Hare K, Brock HW. 1998. Characterization of a Drosophila homologue of the 160-kDa subunit of the cleavage and polyadenylation specificity factor CPSF. Mol Gen Genet Apr;257(6):672-80.

13. Takagaki Y, Manley JL. 2000. Complex protein interactions within the human polyadenylation machinery identify a novel component. Mol Cell Biol 20:1515-25.

14. OConnor MS, Safari A, Liu D, Qin J, and Songyang Z. (2004) The human Rap1 protein complex and modulation of telomere length. *J Biol. Chem*. 279(27):28585-91.

15. Liu D, Safari A, O'Connor MS, Chan DW, Laegeler A, Qin J, Songyang Z. (2004) PTOP interacts with POT1 and regulates POT1 telomeric localization. *Nat. Cell Biol.* 6(7):673-80.

16. Liu D, O'Connor MS, Qin J, Songyang Z. (2004) Telosome, a mammalian telomere-associated complex formed by multiple telomeric proteins. *J Biol. Chem.* 279(49):51338-42.

17. French JD, Dunn J, Smart CE, Manning N, Brown MA. (2005) Disruption of BRCA1 function results in telomere lengthening and increased anaphase bridge formation in immortalized cell lines. Genes Chromosomes Cancer. Nov 10; [Epub ahead of print]

Appendix

Rodriguez M, Yu X, Chen J, and Songyang Z. (2003) Phosphopeptide binding specificities of BRCT domains. *J Biol Chem.* 279:8802-7.

OConnor MS, Safari A, Liu D, Qin J, and Songyang Z. (2004) The human Rap1 protein complex and modulation of telomere length. *J Biol. Chem*. 279(27):28585-91.

Liu D, O'Connor MS, Qin J, Songyang Z. (2004) Telosome, a mammalian telomere-associated complex formed by multiple telomeric proteins. J Biol. Chem. 279(49):51338-42.

THE JOURNAL OF BIOLOGICAL CHEMISTRY
Vol. 278, No. 52, Issue of December 26, pp. 52914–52918, 2003
Printed in U.S.A.

Phosphopeptide Binding Specificities of BRCA1 COOH-terminal (BRCT) Domains*

Received for publication, September 9, 2003, and in revised form, October 16, 2003
Published, JBC Papers in Press, October 24, 2003, DOI 10.1074/jbc.C300407200

Maria Rodriguez‡§, Xiaochun Yu¶§, Junjie Chen¶, and Zhou Songyang‡‖

From the ‡Verna and Marrs McLean Department of Biochemistry and Molecular Biology, Baylor College of Medicine, Houston, Texas 77030 and the ¶Department of Oncology, Mayo Clinic, Rochester, Minnesota 55905

Protein phosphorylation by protein kinases may generate docking sites for other proteins. It thus allows the assembly of signaling complexes in response to kinase activation. Several protein domains that bind phosphoserine or phosphothreonine residues have been identified, including the 14-3-3, PIN1, FHA, KIX, WD-40 domain, and polo box (Yaffe, M. B., and Elia, A. E. (2001) *Curr. Opin. Cell Biol.* 13, 131–138; Elia, A. E., Cantley, L. C., and Yaffe, M. B. (2003) *Science* 299, 1228–1231). The BRCA1 COOH-terminal (BRCT) domains are protein modules found in many proteins that regulate DNA damage responses (Koonin, E. V., Altschul, S. F., and Bork, P. (1996) *Nat. Genet.* 13, 266–268). Whether BRCT domains can mediate phosphorylation-dependent interactions has not been systematically investigated. We report here that the BRCT domains also recognize phosphopeptides. Oriented peptide library analysis indicated that the BRCT domains from BRCA1, MDC1, BARD1, and DNA Ligase IV preferred distinct phosphoserine-containing peptides. In addition, the interaction between BRCA1 and the BRCT binding motif of BACH1 was required for BACH1 checkpoint activity. Furthermore, BRCT domains of the yeast DNA repair protein Rad9 could bind phosphopeptides, suggesting that the BRCT domains represent a class of ancient phosphopeptide-binding modules. Potential targets of BRCT domains were identified through data base search. Structural analysis of BRCA1 BRCT repeats also predicted conserved residues that may form the phosphopeptide-binding pocket. Thus, the BRCT repeats are a new family of phosphopeptide-binding domains in DNA damage responses.

Originally identified as a sequence motif homologous to the BRCA1 COOH-terminal region, the BRCT[1] domain is a protein domain approximately 90 amino acids in length (3–6). It is an ancient protein module that can be found in single cell eukaryotes (7). In the human genome more than 30 BRCT-containing proteins have been documented. Interestingly, most of the BRCT domains associate with proteins involved in DNA repair and cell cycle checkpoint response (5, 6). The exact function of BRCT domains is not yet clear; they have been postulated to mediate protein-protein interactions (7, 8). Heterodimerization between single BRCT domains (*e.g.* XRCC1 and DNA Ligase III) has been reported (9, 10). In addition, BRCT domains of 53BP1 can interact with P53, while BRCT domains of BRCA1 bind DEAH family helicase BACH1 and CtBP interacting protein CTIP (11–13). Interestingly, it was shown that the BRCT domains might also bind double stranded DNA breaks (14).

In addition to heterodimerization of BRCT domains, emerging evidence suggests that BRCT domains may mediate phosphorylation dependent interactions. For example, association of the sixth BRCT domain of TOPBP1 and E2F1 was shown to be regulated by phosphorylation (15). Interactions between BRCA1 and BACH1 depend on BACH1 phosphorylation as well (16). However, whether other BRCT domains can directly binding to phosphopeptide and what the specificities of BRCT domains are remain to be determined.

We were particularly intrigued by the possibility of BRCT domains mediating phosphorylation-dependent interactions, because protein phosphorylation by protein kinases is known to trigger the assembly of phosphorylation-dependent signal complexes critical for cell growth and survival (1, 17). Many protein domains or modules have evolved to mediate such activities. The best examples are the Src homology domain 2 and phosphotyrosine-binding domains that recognize phosphorylated sites by protein-tyrosine kinases in a sequence-specific manner (17, 18). Recently, several protein domains that bind phosphoserine or phosphothreonine residues have been identified, including the 14-3-3, FHA, KIX, PIN1, WD-40, and polo box (1, 2). Notably, each of these domains recognizes a subset of substrates phosphorylated by different protein kinases. For instance, 14-3-3 recognizes sites that are phosphorylated by Arg-directed kinase such as Akt/PKB, while FHA domains bind sites that are substrates of phosphatidylinositol 3-kinase family (1). Given the large number of protein kinases in the human genome, it has been postulated that novel families of phosphopeptide-binding domains that transmit signals from different protein kinases may exist. If BRCT domains can indeed bind phosphopeptides directly, it will provide new insight about how signaling complexes are regulated by DNA damage. To answer such questions, we carried out experiments to study the specificities of BRCT domains using oriented peptide libraries.

MATERIALS AND METHODS

BRCT Domain Constructs and Fusion Proteins—A DNA fragment encoding the human BRCA1 BRCT domain (residues 1599–1863) was cloned into the pGEX-4T1 vector. Constructs of GST BRCT fusions containing human BARD1 (residues 554–777), human MDC1 (residues 2727–3089), human DNA Ligase IV (residues 618–911), and *Saccharomyces cerevisiae* RAD9 (residues 962–1309) were cloned similarly into pGEX-4T1. GST fusion proteins were purified as described previously (19).

Oriented Peptide Library Analysis—Two phosphoserine-containing peptide libraries (X3: ISRSTpS*XXX*NK and X6: KA*XXX*pS*XXX*AK)

* This work was supported by Department of Defense Breast Cancer Idea Award DAMD 17-01-1-0145 (to Z. S.), by the Robert Welch Foundation (to Z. S.), and by Initiative for Minority Student Development Grant GM569209 (to M. R.). The costs of publication of this article were defrayed in part by the payment of page charges. This article must therefore be hereby marked "*advertisement*" in accordance with 18 U.S.C. Section 1734 solely to indicate this fact.

§ These authors contributed equally.

‖ To whom correspondence should be addressed: Verna and Marrs McLean Dept. of Biochemistry and Molecular Biology, Baylor College of Medicine, One Baylor Plaza, Houston, TX 77030. E-mail: songyang@bcm.tmc.edu.

[1] The abbreviations used are: BRCT, BRCA1 COOH-terminal; GST, glutathione *S*-transferase; FHA, forkhead-associated; FITC, fluorescein isothiocyanate; siRNA, small interfering RNA.

were synthesized as described previously (19), where *X* is any amino acids except Cys. For library analysis, 1 mg of the peptide library was incubated with 100–300 μg of GST BRCT-agarose beads. Then the beads were washed five times with 2 ml of phosphate-buffered saline. The bound peptides were eluted with 30% acetic acids, lyophilized, and sequenced on an ABI 477 peptide sequencer. Relative selectivities of amino acids at each degenerate position were calculated as described previously (19).

SPOT Peptide Array Synthesis and Screen—The BACH1 peptide array was synthesized on cellulose membrane using the ASP222 SPOT robot (20). The parental peptide SRSTpSPTFNK was scanned with 19 of the 20 amino acids (except Cys), phosphoserine, and phosphothreonine. The array membrane was first blocked with 3% bovine serum albumin in TBST (0.1 M Tris-HCl, pH 7.4, 150 mM NaCl, 0.1% Tween 20) for 2 h at room temperature. GST-BRCT of BRCA1 (3 μg) was labeled with anti-GST-horseradish peroxidase (Amersham Biosciences) (0.75 μg) for 30 min at room temperature. The fusion proteins were then added to the array membrane at a final concentration of 2 μg/ml for 30 min. The array membrane was subsequently washed with TBST for 10 min three times. GST-BRCT bound peptide spots were visualized by ECL.

Affinity Measurements Using Fluorescence Polarization—A FITC-labeled phosphopeptide with the sequence VDDpSYVFNK was first synthesized. For controls, an aliquot of this peptide was dephosphorylated with alkaline phosphatase. The phosphopeptide or dephosphorylated peptide was incubated with different concentration of BRCA1 GST-BRCT fusion proteins in a 96-well plate. Fluorescence polarization was measured on TECAN Polarion.

BACH1 siRNA and siRNA-resistant BACH1—BACH1 siRNA (AGCUUACCCGUCACAGCUUdTdT) was transfected into cells by Oligofectamine (Invitrogen). SiRNA-resistant (silent) mutants of wild-type BACH1 and BACH1 BRCT-binding mutants (T989A, S990A, or F993A) were created by substituting four nucleotides in the BACH1 siRNA targeting region (G69T, T70A, C71G, A72C). All BACH1 constructs were cloned into the pCDNA 3.1 His/Myc vector (Invitrogen). Immunoprecipitation and immunoblotting were carried out as described previously (16).

G_2/M Checkpoint Assay—For assaying BACH1 activity, cells were transfected with BACH1 mutant constructs immediately after siRNA transfection with LipofectAMINE 2000 (Invitrogen). At 48 h after transfection, cells were exposed to 10-Gy γ-irradiation, allowed to recover for 3 h, and then treated with nocodazole (1 μg/ml) for 15 h. Cells were fixed with 3% paraformaldehyde and stained with rabbit anti-phospho-histone H3 antibody, followed by incubation with rhodamine-conjugated secondary antibody. Mutant BACH1 was stained with anti-myc antibody (9E10), followed by FITC-conjugated secondary antibody. The BACH1 mutants were expressed in ~90% of the cells based on immunofluroscence microscopy. The phospho-histone H3-positive staining cells were examined by immunofluroscence microscopy.

RESULTS

The BRCA1 BRCT Domains Recognize Phosphopeptides with the Phosphoserine-Aromatic-Hydrophobic-Phe Motif—One of the known *in vivo* targets of BRCA1 is BACH1, a member of the DEAH helicase family (13). In the course of mapping BRCA1 and BACH1 interactions, we found that tandem but not individual BRCA1 BRCT domains directly bound BACH1 in a phosphorylation-dependent manner (16). Further analysis of BRCA1 and BACH1 interaction demonstrated that BRCA1 BRCT domains specifically recognize phosphorylated Ser^{990} (ISRSTS^{990}PTFNK) of BACH1. These data suggested that the BRCT domain may be a phosphopeptide-binding module.

To understand the sequence binding preference of BRCT domains, we first examined the specificity of BRCA1 BRCT domain using an oriented peptide library (19). The phosphoserine containing peptide library X3 (ISRSTpS*XXX*NK) was synthesized, based on the sequence surrounding residue Ser^{990} of human BACH1. Using this phospho-library, we found that BRCA1 BRCT domains preferred aromatic amino acids at the P+1 position and aromatic/hydrophobic residues at the P+2 position (Fig. 1). Notably, at the P+3 position COOH-terminal to the phosphoserine, Phe is strongly selected, indicating that Phe at this position is critical for recognition by the BRCA1 BRCT domains. Thus, BRCA1 BRCT domains prefer a phosphoserine-aromatic-hydrophobic-Phe motif.

To further examine the specificity of BRCA1 BRCT domain at residues NH_2-terminal to the phosphoserine, the phospho-library X6 with the sequence KA*XXX*pS*XXX*AK was used. As shown in Table I, the BRCA1 BRCT domains preferred a [YE]-E-[TV]-pS-[YFH]-[VTYF]-[FY] motif with weak selection at the NH_2 terminus, suggesting that residues COOH-terminal to phosphoserine are important for binding to BRCA1 BRCT domains. A BRCA1 BRCT binding peptide (VDDpSYVFNK) was then synthesized, and its affinity to BRCA1 BRCT domains was measured. Indeed, this peptide bound with an affinity of 162 nM to the BRCA1 BRCT domains. In addition, such interaction was dependent on phosphorylation, as the unphosphorylated control peptide failed to bind (Fig. 2*A*).

To further probe the binding motif for BRCA1 BRCT domains, we generated an array of phosphopeptides based on the

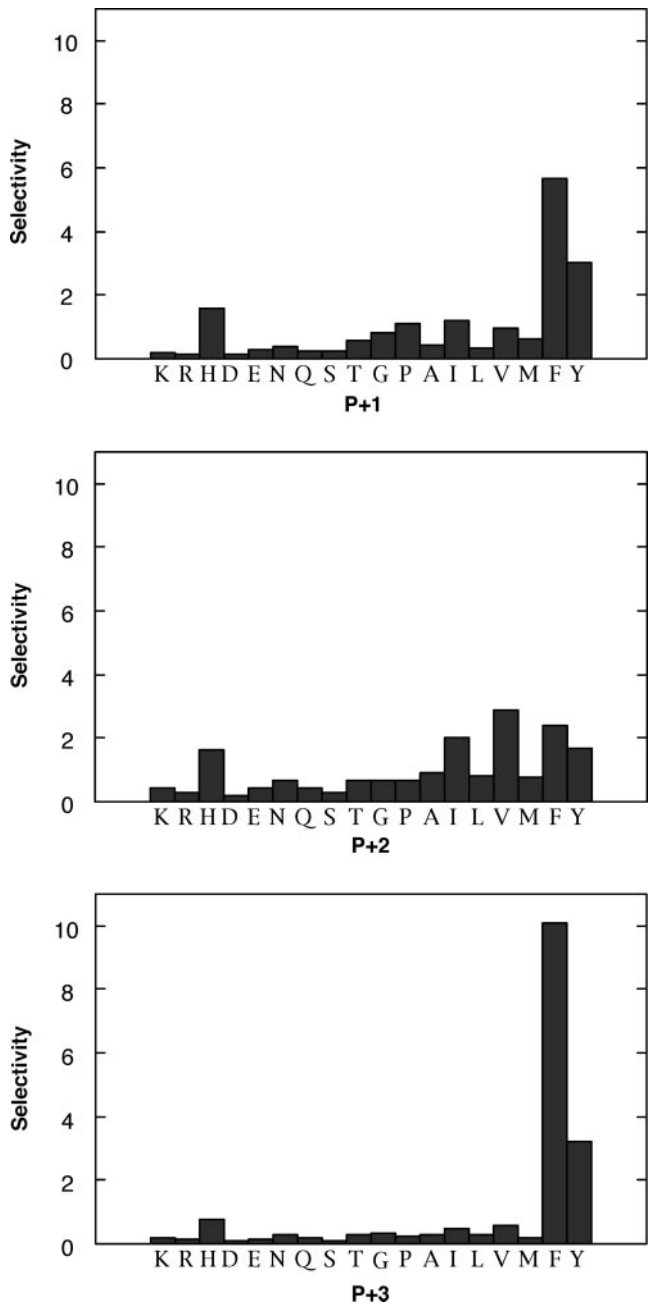

FIG. 1. **The BRCT repeats of BRCA1 recognize specific phosphoserine-containing peptides.** The binding specificity of BRCA1 BRCT domains was determined using an oriented peptide library ISRSTpS*XXX*NK. Relative selections of individual amino acids at position COOH-terminal to phosphoserine (P+1, +2, and +3) were shown here. A value smaller than 1 indicates that the amino acid is not preferred. Trp was not included due to peptide sequencing problems.

TABLE I
The specificities of BRCT domains

BRCT domains	Selectivity positions						
	−3	−2	−1	0	+1	+2	+3
BRCA1X3 Lib				pS	F (5.7) Y (3.0) H (1.6)	V (2.9) F (2.3) I (2.0) Y (1.7) H (1.7)	F (10.1) Y (3.2)
BRCA1 X6 Lib	Y (1.4) E (1.3)	E (1.4)	T (1.3) V (1.3)	pS	Y (2.6) F (2.3) H (1.3)	V (2.2) T (1.5) Y (1.5) F (1.4)	F (5.1) Y (1.5)
MDC1 X3 Lib				pS	I (2.4) P (1.7) V (1.6) F (1.6) Y (1.3)	E (4.0) V (2.9) D (2.1) I (1.3)	Y (5.6) F (2.0) E (1.9) I (1.3)
BARD1 X3 Lib				pS	D (1.7) E (1.4)	D (2.0) E (1.3)	E (2.2)
LIG IV X3 Lib				PS	Y (2.6) A (1.4) D (1.4) L (1.3)	Y (1.9) A (1.5) D (1.3)	I (1.6) Y (1.4) D (1.4)
RAD9 X3 Lib				PS	Y (2.2) L (1.6) I (1.5)	I (1.8) Y (1.5) L (1.5) K (1.3)	I (2.4) L (1.4) K (1.4)

BACH1 peptide using the SPOT peptide synthesizer. Consistent with our finding that Phe at P+3 is crucial for binding, substitution with amino acids other than Phe at P+3 abolished BRCA1 BRCT interaction (Fig. 2*B*). Similarly, only β-branched amino acids (Thr, Val, and Ile) were tolerated at the P+2 position. This result recapitulated our oriented peptide library data and again highlighted the importance of the P+3 position for recognition by the BRCA1 BRCT domain. The oriented peptide library and SPOT array data collectively demonstrate that the BRCT domains from BRCA1 recognize specific phosphorylated sequences with the consensus motif phosphoserine-aromatic-hydrophobic-Phe motif.

The BRCT-binding Motif of BACH1 Is Important for BRCA1-dependent G_2/M Checkpoint Control—BRCA1/BACH1 interaction is important for DNA damage-induced checkpoint control during G_2 to M cell cycle transition (16). To test whether the BRCA1-binding motif of BACH1 identified by *in vitro* studies is involved in this process, we used a γ-ray-induced G_2/M checkpoint assay.

First, we constructed Thr^{989}-to-Ala (T989A), Ser^{990}-to-Ala (S990A), or Phe^{993}-to-Ala mutants of BACH1. BACH1 siRNA-resistant forms of wild-type and mutant BACH1 were then generated by introducing silent mutations in the siRNA target region. All these BACH1 proteins were expressed in HeLa cells. However, only wild-type BACH1 and the T989A mutant, but not the S990A or F993A mutant, were associated with BRCA1 (Fig. 3*A*). This result indicates that the BRCA1 binding-motif of BACH1, especially P+3 Phe, is necessary for BRCA1/BACH1 interaction *in vivo*. To explore the *in vivo* functional link between the BRCT-binding motif of BACH1 and BRCA1 BRCT domains, HeLa cells were treated with BACH1 siRNA and then transfected with siRNA-resistant BACH1 or BACH1 mutants. BACH1 siRNA repressed the expression of endogenous BACH1 but not exogenous siRNA-resistant BACH1 (Fig. 3*B*). Cells treated with BACH1 siRNA showed G_2/M checkpoint defect after DNA damage (Fig. 3*C*). While expression of wild-type BACH1 and the T989A mutant rescued the checkpoint defect, the S990A and F993A mutants had no effect (Fig. 3, *D* and *E*). These data further confirm P+3 Phe as a key residue for BRCA1 BRCT and BACH1 interaction and indicate that the

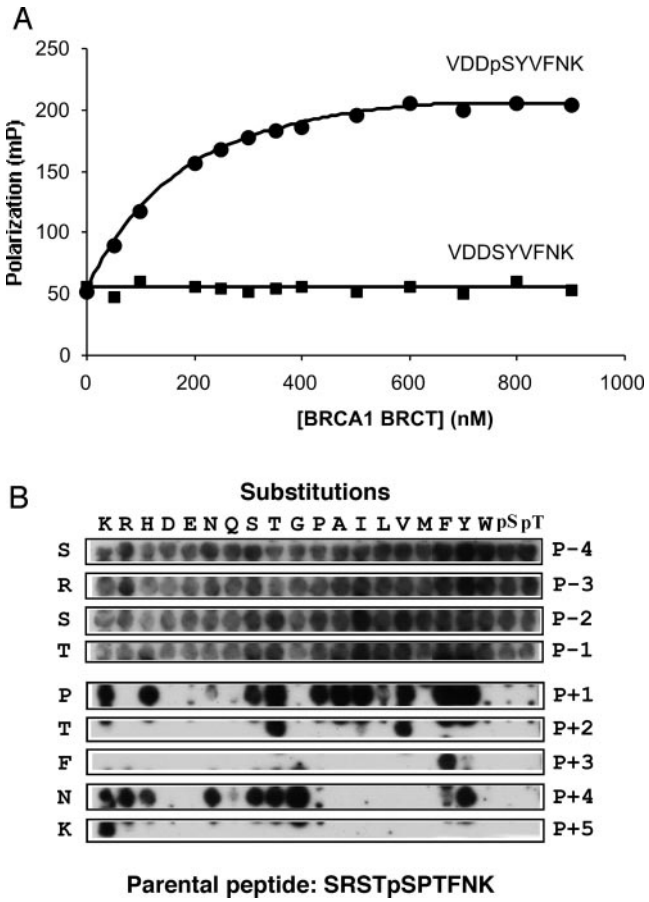

FIG. 2. **BRCA1 BRCT domains bind phosphopeptides with the phosphoserine-aromatic-hydrophobic-Phe motif.** *A*, fluorescence polarization analysis of phosphopeptide binding to BRCA1 BRCT domains. FITC-labeled phosphorylated VDDpSYVFNK (*circles*) or unphosphorylated VDDSYVFNK peptide (*squares*) (20 nM) was incubated with different concentrations of GST-BRCT tandem domains. Fluorescence polarization was then measured. *B*, amino acid scan of BACH1 S990 peptide. The parental BACH1 phosphopeptide SRSTpSPTFNKA and its derivatives were synthesized on cellulose membrane. At each position (P−4 to P+5), the parental residue was substituted by one of the 20 amino acids (except Cys), phosphoserine, and phosphothreonine. The membrane then was probed with GST-BRCA1 BRCT domains and anti-GST-horseradish peroxidase.

BRCA1 binding-motif of BACH1 is important for the function of BRCA1 BRCT domain *in vivo*.

The Specificities of BRCT Domains of MDC1, BARD1, and Ligase IV—To investigate whether other BRCT domains can also bind phosphopeptides, we studied the specificities of several BRCT domains. Interestingly, tandem BRCT domains from MDC1, BARD1, and Ligase IV specifically bound phosphopeptides in the X3 library (Table I).

MDC1 is a recently identified mediator of DNA damage responses (21–26). MDC1 contains two BRCT repeats at its carboxyl terminus. Using the X3 library, we found that MDC1 BRCT domains selected a distinct set of phosphopeptides compared with BRCA1. Instead of Phe, Tyr is the most selected amino acid by MDC1 at the P+3 position (Table I). At the P+2 position, acidic residues Glu and Asp were selected in addition to Val and Ile. At the P+1 position hydrophobic residues are preferred. Thus, the MDC1 BRCT domains bind phosphopeptides with the motif pS-hydrophobic-[EVDI]-[YF].

BARD1 is a cancer susceptible protein that is mutated in families of breast cancer patients (27). BARD1 has an NH_2-terminal ring finger domain which heterodimerizes with BRCA1 and two COOH-terminal BRCT domains with unknown function (4). Oriented peptide library analyses indicated

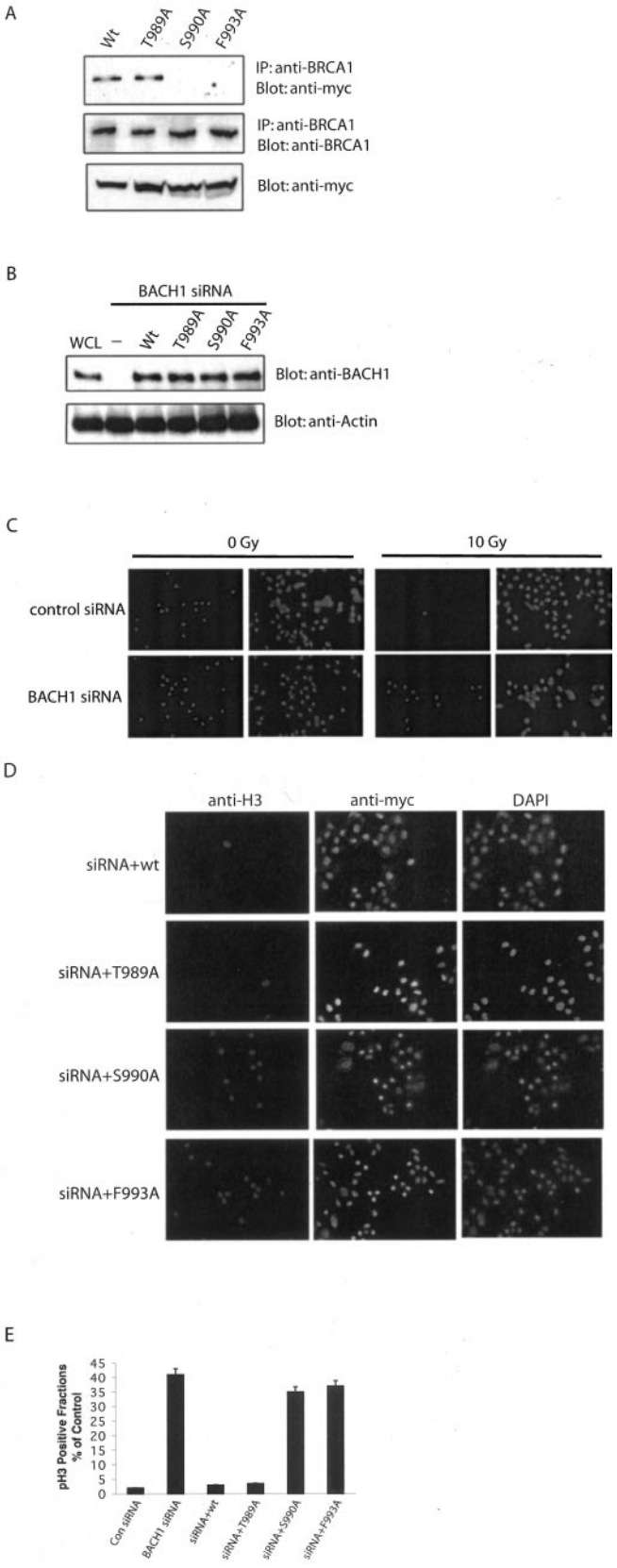

FIG. 3. **The BRCT-binding motif of BACH1 is required for BRCA1-dependent G_2/M checkpoint control.** *A*, siRNA resistant BACH1 mutants were expressed in HeLa cells. Immunoprecipitation and immunoblotting were done with anti-BRCA1 or anti-myc antibodies as indicated. *B*, HeLa cells were transfected with BACH1 siRNA and siRNA-resistant BACH1 mutants. Whole cell lysates were blotted with anti-BACH1 or anti-actin antibodies. *C*, G_2/M checkpoint was detected in BACH1 siRNA-treated cells. Checkpoint assays were described under "Material and Methods." *D*, wild-type and T989A of BACH1 siRNA-resistant mutants rescued the G_2/M checkpoint defect generated by BACH1 siRNA but not the S990A or F993A mutant. *E*, the fraction of M phase cells from *C* and *D* is expressed as a percentage of that measured in non-irradiated control cells.

TABLE II
Potential targets of BRCA1 and MDC1 BRCT repeats in Swiss-Prot
Selected nuclear targets are shown.

BRCT domains	Searched motif	Predicted targets	Sequence
BRCA1	pS-[FYIVPAKHST]-[VT]-F-[GSTNYRKH]	BACH1	SRST**S**PTFNK
		BRCA1	IKES**S**AVFSK
		Kinesin-like KIF1B	DRTP**S**PTFST
		Protein Kinase NIK	SQEF**S**PTFSE
		CTIP	TRVS**S**PVFGA
		Msh3	LHSE**S**SVFGQ
		Nuclear pore Nup153	SAGS**S**FVFGT
		repressor CTCFL	CRYC**S**AVFHE
		hTid-1	RVQK**S**PVFRR
		NCoA-2	PRRN**S**HTFNC
		NCoA-3/SRC-3	QRQK**S**HTFNC
		RNA-binding protein 12	ASFG**S**PTFSS
MDC1	pS-[IVFP]-[EDVI]-Y	HDAC8	DHPD**S**IEYGL
		HDAC10	GLVH**S**PEYVS
		CENP-C	KSEE**S**PVYSN
		MDM2	STSS**S**IIYSS
		RNA Polymerase II	YSPS**S**PEYTP
		WRN helicase	EFTG**S**IVYSY
		ERCC-6	MDGA**S**PDYVL
		Fanconi anemia FACF	HPAL**S**PVYLG
		GATA-4	GAAS**S**PVYLP
		KIAA0076	HMLS**S**PDYQI
RAD9	pS-[YILQP]-I-I	RAD1	EMMP**S**YIIMF
		RFC5	LKSS**S**PIIKP
		MEC1	HQLY**S**QIISN
		PDS5	LFRA**S**PIIYN
		RAD50	KVLA**S**IIIRL
		Helicase MER3	EKKQ**S**QIIDR
		Helicase DNA2	TYSF**S**IIICN
		CDC68	DWTY**S**PIIQS
		CDC45	NIFG**S**QIIQC
		RNA helicase DHR1	TKYS**S**IIIDE
		SMC2	ANPS**S**QIIAR

that the tandem BRCT domains of BARD1 specifically recognize Asp/Glu residues at the P+1, +2, and +3 positions (Table I). The selection for Asp at the P+2 and Glu at the P+3 seemed most critical for BARD1 BRCT domain binding. Thus, the binding motif for BARD1 BRCT domains is pS-[DE]-[DE]-E.

DNA Ligase IV functions to join single-strand breaks in double-stranded DNA (28, 29). It plays a major role in V(D)J recombination and non-homologous end joining. At the COOH terminus of Ligase IV are two BRCT domains. Different from MDC1 and BARD1, Ligase IV BRCT repeats preferred to bind phosphopeptides with Tyr and Ile, respectively, at the P+1 and P+3 positions (Table I). These results demonstrated that the BRCT domains are protein modules that recognize specific phosphopeptides.

S. cerevisiae RAD9 BRCT Domains Bind Phosphopeptides—The BRCT domain is an ancient structural fold that can be traced back to bacteria. In bacteria and fungi, BRCT domains are also frequently found in proteins that regulate DNA damage responses. We therefore were interested in determining if BRCT domains from single cell eukaryotes could bind phosphopeptides as well. One of the proteins we studied is budding yeast RAD9, which is essential for cell cycle checkpoint control (30). As shown in Table I, the tandem BRCT domains of RAD9 preferred Tyr at the P+1 position, and Ile at the P+2 and P+3 positions. Thus, the RAD9 BRCT repeats recognize phosphopeptides with the motif pS-Y-I-I. This result suggests that BRCT domains have

evolved as a phosphopeptide-binding module early in evolution.

Prediction of Potential in Vivo Targets of BRCT Domains—To identify potential targets of BRCT domains, we performed pattern searches in Swiss-Prot using the consensus motifs from our library and SPOT array analyses (Table II). Some of the interesting predicted targets for BRCA1 include BRCA1 itself, kinesin-like protein KIF1B, mismatch repair protein Msh3, Rb-binding protein CTIP, co-repressor NCoA-2 and NCoA-3/SRC-3. For MDC1, histone deacetylases HDAC8, and HDAC10, GATA family transcription factors could be potential targets. Interestingly, RNA polymerase II contains repeats of the MDC1-binding motif. A search of potential targets of RAD9 in budding yeast also found a short list of proteins that regulate DNA repair and cell cycle. Notably these include MEC1, RAD1, and RFC p140, which have been shown to interact with RAD9 genetically and biochemically.

DISCUSSION

Tandem Versus Single BRCT Domains—Our results have shown that tandem BRCT repeats can specifically recognize phosphoserine containing peptides, suggesting that the BRCT domain represents a new class of modules that mediate phosphorylation dependent protein-protein interactions. Most BRCT domain-containing proteins are known to mediate DNA damage responses (5, 6). These proteins are often recruited to the sites of DNA damage, coinciding with the activation of protein kinases such as ATM, ATR, Chk1, and Chk2 (31–33). The identification of BRCT domains as phosphopeptide-interacting motifs suggest that BRCT domains may facilitate the assembly of signaling complexes that sense the activation of damage and checkpoint kinases. In fact, numerous residues in the BRCA1 BRCT repeats are mutated in breast cancer cells (34, 35). Some of these mutations may disrupt the ability of BRCT domains to bind phosphorylated cellular target and therefore contribute to disease phenotypes.

There is one notable difference between BRCT and other phosphopeptide-binding domains such as Src homology domain 2 and FHA domains. Among the BRCT domains we examined so far, only tandem but not single BRCT domains bound a sufficient amount of phosphopeptides from the peptide library. It is possible that inter-BRCT interactions is required for phosphopeptide binding, or tandem BRCTs function as a unit to bind phosphopeptides. In fact, structural studies have revealed that tandem BRCTs may have evolved from a common ancestor, because the linker structures between the two BRCT domains are also conserved (36). In further support of this idea, single point mutations in either of the two repeats in BRCA1 can abolish its interaction with BACH1 (13). Our data, however, do not rule out that single BRCT domains can also bind phosphopeptides. Interestingly, single BRCT domains (*e.g.* XRCC1 and Ligase III) have been shown to form heterodimers. One intriguing possibility may exist that such heterodimers may function as a phosphopeptide-binding unit.

Structural Insight into BRCT Phosphopeptide Recognition—The structures of several BRCT domains have been determined (8, 13, 36–38). These studies indicate that the BRCT domain consists of four-stranded parallel β sheets bundled by three α helices. The two BRCT repeats of BRCA1 connected by the linker region are arranged in tandem (36). It is possible that similar to 14-3-3 and FHA, the phosphoserine-binding pocket of BRCT repeats may be formed by conserved Arg or Lys residues (39, 40). Secondary structure comparisons of BRCA1 BRCT repeats from several different species suggested that Lys^{1667}, Arg^{1670}, Lys^{1671}, Lys^{1724}, Arg^{1726}, Lys^{1727}, Arg^{1737}, Lys^{1750}, Arg^{1751}, Arg^{1753}, and Lys^{1759} on human BRCA1 are highly conserved. In addition, positive charged residues are found at similar positions on BRCT domains of MDC1, BARD1, and DNA Ligase IV. It is interesting to note that these Arg/Lys residues are mainly located at two regions of BRCA1 BRCT domains. One region is on the surface of BRCT domain structure formed by Lys^{1667}, Arg^{1670}, and Lys^{1671} located on the helix α1A, and Arg^{1726} and Lys^{1727} located on the loop between α3A and α4A. The second region is near the connecting linker of the tandem BRCTs. These regions may form the phosphoserine-binding pocket of BRCA1 BRCT repeats. In support of this model, mutation of several residues in the second region of the BRCA1 BRCT repeats significantly decreased BACH1 binding *in vitro*, suggesting that the phosphopeptide-binding pocket may reside in this region as well (36).

Acknowledgments—We thank Dr. Dan Liu for critical reading of this manuscript and Dr. John McMurray for technical assistance.

REFERENCES

1. Yaffe, M. B., and Elia, A. E. (2001) *Curr. Opin. Cell Biol.* **13,** 131–138
2. Elia, A. E., Cantley, L. C., and Yaffe, M. B. (2003) *Science* **299,** 1228–1231
3. Koonin, E. V., Altschul, S. F., and Bork, P. (1996) *Nat. Genet.* **13,** 266–268
4. Wu, L. C., Wang, Z. W., Tsan, J. T., Spillman, M. A., Phung, A., Xu, X. L., Yang, M. C., Hwang, L. Y., Bowcock, A. M., and Baer, R. (1996) *Nat. Genet.* **14,** 430–440
5. Bork, P., Hofmann, K., Bucher, P., Neuwald, A. F., Altschul, S. F., and Koonin, E. V. (1997) *FASEB J.* **11,** 68–76
6. Callebaut, I., and Mornon, J. P. (1997) *FEBS Lett.* **400,** 25–30
7. Aravind, L., Walker, D. R., and Koonin, E. V. (1999) *Nucleic Acids Res.* **27,** 1223–1242
8. Zhang, X., Morera, S., Bates, P. A., Whitehead, P. C., Coffer, A. I., Hainbucher, K., Nash, R. A., Sternberg, M. J., Lindahl, T., and Freemont, P. S. (1998) *EMBO J.* **17,** 6404–6411
9. Taylor, R. M., Wickstead, B., Cronin, S., and Caldecott, K. W. (1998) *Curr. Biol.* **8,** 877–880
10. Caldecott, K. W., McKeown, C. K., Tucker, J. D., Ljungquist, S., and Thompson, L. H. (1994) *Mol. Cell. Biol.* **14,** 68–76
11. Chai, Y. L., Cui, J., Shao, N., Shyam, E., Reddy, P., and Rao, V. N. (1999) *Oncogene* **18,** 263–268
12. Yu, X., Wu, L. C., Bowcock, A. M., Aronheim, A., and Baer, R. (1998) *J. Biol. Chem.* **273,** 25388–25392
13. Cantor, S. B., Bell, D. W., Ganesan, S., Kass, E. M., Drapkin, R., Grossman, S., Wahrer, D. C., Sgroi, D. C., Lane, W. S., Haber, D. A., and Livingston, D. M. (2001) *Cell* **105,** 149–160
14. Yamane, K., and Tsuruo, T. (1999) *Oncogene* **18,** 5194–5203
15. Liu, K., Lin, F. T., Ruppert, J. M., and Lin, W. C. (2003) *Mol. Cell. Biol.* **23,** 3287–3304
16. Yu, X., Chini, C., He, M., Mer, G., and Chen, J. (2003) *Science* **302,** 639–642
17. Pawson, T., and Scott, J. D. (1997) *Science* **278,** 2075–2080
18. Songyang, Z. (1999) *Prog. Biophys. Mol. Biol.* **71,** 359–372
19. Songyang, Z., Shoelson, S. E., Chaudhuri, M., Gish, G., Pawson, T., Haser, W. G., King, F., Roberts, T., Ratnofsky, S., Lechleider, R. J., and B. G. Neel, Birge, R. B., Fajardo, J. E., Chou, M. M., Hanafusa, H., Schaffhausen, B., and Cantley, L. C. (1993) *Cell* **72,** 767–778
20. Frank, R. (2002) *J. Immunol. Methods* **267,** 13–26
21. Ozaki, T., Nagase, T., Ichimiya, S., Seki, N., Ohiri, M., Nomura, N., Takada, N., Sakiyama, S., Weber, B. L., and Nakagawara, A. (2000) *DNA Cell Biol.* **19,** 475–485
22. Peng, A., and Chen, P. L. (2003) *J. Biol. Chem.* **278,** 8873–8876
23. Stewart, G. S., Wang, B., Bignell, C. R., Taylor, A. M., and Elledge, S. J. (2003) *Nature* **421,** 961–966
24. Xu, X., and Stern, D. F. (2003) *J. Biol. Chem.* **278,** 8795–8803
25. Lou, Z., Minter-Dykhouse, K., Wu, X., and Chen, J. (2003) *Nature* **421,** 957–961
26. Goldberg, M., Stucki, M., Falck, J., D'Amours, D., Rahman, D., Pappin, D., Bartek, J., and Jackson, S. P. (2003) *Nature* **421,** 952–956
27. Thai, T. H., Du, F., Tsan, J. T., Jin, Y., Phung, A., Spillman, M. A., Massa, H. F., Muller, C. Y., Ashfaq, R., Mathis, J. M., Miller, D. S., Trask, B. J., Baer, R., and Bowcock, A. M. (1998) *Hum. Mol. Genet.* **7,** 195–202
28. Timson, D. J., Singleton, M. R., and Wigley, D. B. (2000) *Mutat. Res.* **460,** 301–318
29. Tomkinson, A. E., and Levin, D. S. (1997) *BioEssays* **19,** 893–901
30. Weinert, T. A., and Hartwell, L. H. (1990) *Mol. Cell. Biol.* **10,** 6554–6564
31. Shiloh, Y. (2001) *Curr. Opin. Genet. Dev.* **11,** 71–77
32. Khanna, K. K., and Jackson, S. P. (2001) *Nat. Genet.* **27,** 247–254
33. Pierce, A. J., Stark, J. M., Araujo, F. D., Moynahan, M. E., Berwick, M., and Jasin, M. (2001) *Trends Cell Biol.* **11,** S52—S59
34. Arver, B., Du, Q., Chen, J., Luo, L., and Lindblom, A. (2000) *Semin. Cancer Biol.* **10,** 271–288
35. Rosen, E. M., Fan, S., Pestell, R. G., and Goldberg, I. D. (2003) *J. Cell. Physiol.* **196,** 19–41
36. Joo, W. S., Jeffrey, P. D., Cantor, S. B., Finnin, M. S., Livingston, D. M., and Pavletich, N. P. (2002) *Genes Dev.* **16,** 583–593
37. Krishnan, V. V., Thornton, K. H., Thelen, M. P., and Cosman, M. (2001) *Biochemistry* **40,** 13158–13166
38. Williams, R. S., Green, R., and Glover, J. N. (2001) *Nat. Struct. Biol.* **8,** 838–842
39. Durocher, D., Taylor, I. A., Sarbassova, D., Haire, L. F., Westcott, S. L., Jackson, S. P., Smerdon, S. J., and Yaffe, M. B. (2000) *Mol. Cell* **6,** 1169–1182
40. Rittinger, K., Budman, J., Xu, J., Volinia, S., Cantley, L. C., Smerdon, S. J., Gamblin, S. J., and Yaffe, M. B. (1999) *Mol. Cell* **4,** 153–166

THE JOURNAL OF BIOLOGICAL CHEMISTRY
Vol. 279, No. 27, Issue of July 2, pp. 28585–28591, 2004

Printed in U.S.A.

The Human Rap1 Protein Complex and Modulation of Telomere Length*

Received for publication, November 26, 2003, and in revised form, March 19, 2004
Published, JBC Papers in Press, April 20, 2004, DOI 10.1074/jbc.M312913200

Matthew S. O'Connor, Amin Safari, Dan Liu, Jun Qin, and Zhou Songyang‡

From the Verna and Marrs McLean Department of Biochemistry and Molecular Biology, Baylor College of Medicine, Houston, Texas 77030

Proper maintenance of telomere length and structure is necessary for normal proliferation of mammalian cells. Mammalian telomere length is regulated by a number of proteins including human repressor activator protein (hRap1), a known association factor of TRF2. To further delineate hRap1 function and its associated proteins, we affinity-purified and identified the hRap1 protein complex through mass spectrometry analysis. In addition to TRF2, we found DNA repair proteins Rad50, Mre11, PARP1 (poly(ADP-ribose) polymerase), and Ku86/Ku70 to be in this telomeric complex. We demonstrated by deletional analysis that Rad-50/Mre-11 and Ku86 were recruited to hRap1 independent of TRF2. PARP1, however, most likely interacted with hRap1 through TRF2. Interestingly, knockdown of endogenous hRap1 expression by small hairpin interference RNA resulted in longer telomeres. In addition, overexpression of full-length and mutant hRap1 that lacked the BRCA1 C-terminal domain functioned as dominant negatives and extended telomeres. Deletion of a novel linker domain of hRap1 (residues 199–223), however, abolished the dominant negative effect of hRap1 overexpression. These results indicate that hRap1 negatively regulates telomere length *in vivo* and suggest that the linker region of hRap1 may modulate the recruitment of negative regulators of telomere length.

Telomere-binding proteins TRF1 and TRF2 play pivotal roles in telomere protection and maintenance in mammalian cells (1–5). Several proteins have been shown to associate with TRF1 and TRF2 (3, 5, 6). Recently, a novel telomere regulator human repressor activator protein (hRap1)[1] was identified as a protein that specifically interacts with TRF2 (7). hRap1 is the human homologue of yeast RAP1. In yeast, RAP1 is a negative regulator of telomere length as well as a regulator of transcription (for review, see Refs. 8–13). The RAP1 mutants in *Saccharomyces cerevisiae* (scRAP1) and *Schizosaccharomyces pombe* (spRAP1) are defective in telomere length control and telomere position effects (14–16). In human cells overexpression of hRap1 extends telomeres (7, 17). It has yet to be fully determined, however, whether endogenous hRap1 is a negative or positive regulator of telomere length.

scRAP1 contains two Myb domains and binds telomeric DNA (18, 19). scRAP1 has been shown to recruit Rif1, Rif2, and Sir proteins to regulate telomere length, structure, and transcriptional silencing (11, 20). Whether similar proteins, as found with yeast RAP1, are complexed with hRap1 remains unknown. In contrast, spRAP1 has only one Myb domain and is recruited to telomeres through Taz1, a yeast homologue of TRF2 (15). Similar to spRAP1, hRap1 also contains a single Myb domain without detectable DNA binding activity (7, 21). In addition to the Myb domain, hRap1 has three putative protein-protein interaction domains; they are a BRCT domain, a coiled-coil domain, and a TRF2 interacting RCT domain (7). The function of the hRap1 BRCT and coiled-coil domains has yet to be described.

TRF2 has been shown to associate with the MRN complex (Rad-50, Mre-11, and NBS1) (22). In *S. cerevisiae*, the MRX complex (equivalent of MRN in mammals) has exonuclease activity, is a positive regulator of telomeres, and is responsible for telomere end processing (23–25). Although both scRAP1 and the MRX complex localize to the telomere, the MRX complex does so independent of scRap1 (24, 25). It is possible that hRap1 may interact with the mammalian MRN components, and this association may be necessary for telomere length control. Alternatively, hRap1 and TRF2 may recruit proteins other than the MRN complex to modulate telomere length.

To address these questions, we undertook biochemical approaches to isolate and study protein complexes that are involved in telomere maintenance. We found several DNA repair proteins in addition to TRF2 to be in the hRap1 complex through affinity purification experiments. Furthermore, a more detailed analysis of hRap1 via RNA interference (26, 27) and deletion experiments suggest that hRap1 negatively modulates telomere length *in vivo* and that multiple proteins may be required for hRap1 function.

MATERIALS AND METHODS

Generation of Constructs and Cell Lines of hRap1 and Its Deletion Mutants—Full-length hRap1 was amplified from a HeLa cDNA library and cloned into the pBabe-puro retroviral vector. hRap1 truncations were generated by PCR using *Pfu* Turbo DNA polymerase (Stratagene) from full-length hRap1 and cloned into the pBabe retroviral vector. Constructs were named hRap1 (full-length, amino acids 1–399), ΔMyb (amino acids 1–132 and 192–399), ΔLink (amino acids 1–198 and 224–399), ΔRCT (amino acids 1–290, with an N-terminal nuclear localization signal PRRK), ΔRΔC (ΔRCT/ΔCoil-Coil, amino acids 1–227, with an N-terminal nuclear localization signal PRRK), and ΔBRCT (amino acids 129–399). Full-length and mutant hRap1 are tagged with FLAG epitopes at both the N and C termini. The retroviral vectors were used to transfect BOSC23 cells by the calcium phosphate method to produce retroviruses for subsequent infection of HeLa S3, HT1080, or HTC75

* This work was supported by National Institutes of Health Grant CA84208 (to Z. S.) and by Department of Defense Grant DAMD 17-01-1-0145 (to Z. S.). The costs of publication of this article were defrayed in part by the payment of page charges. This article must therefore be hereby marked "*advertisement*" in accordance with 18 U.S.C. Section 1734 solely to indicate this fact.

‡ To whom correspondence should be addressed: Verna and Marrs McLean Department of Biochemistry and Molecular Biology, Baylor College of Medicine, One Baylor Plaza, Houston, TX 77030. Tel.: 713-798-5220; Fax: 713-796-9438; E-mail: songyang@bcm.tmc.edu.

[1] The abbreviations used are: hRap1, human repressor activator protein; scRAP1, *S. cerevisiae* Rap1; spRAP1, *Schizosaccharomyces pombe* Rap1; BRCT, BRCA1 C-terminal domain; RCT, Rap1 C-terminal domain; MRN, Mre11/Rad50/Nbs1 complex; shRNA, small hairpin interference RNA; mU6, mouse U6; PARP1, poly(ADP-ribose) polymerase.

cells (28). To generate cells stably expressing hRap1 and its mutants, human HeLa S3 and HT1080 cells were infected with the hRap1 retroviruses. These cells were selected with 2 μg/ml puromycin after infection for 3 days to obtain cells stably expressing hRap1 and its mutants.

Preparation of Nuclear Extracts—HeLa S3 cells stably expressing FLAG-tagged hRap1 or mutants were grown in suspension up to 1×10^6 cells/ml. A total of $1–6 \times 10^9$ cells were collected for nuclear extract preparation. Briefly, cells were washed in cold phosphate-buffered saline and hypotonic buffer (10 mM Tris, pH 7.3, 10 mM KCl, 1.5 mM $MgCl_2$, 0.2 mM phenylmethylsulfonyl fluoride and 10 mM 2-mercaptoethanol), allowed to swell for 15 min in hypotonic buffer, and homogenized until cell membrane lysis was ~80% complete. Cells were resuspended in low salt buffer (20 mM KCl, 20 mM Tris, pH 7.3, 25% glycerol, 1.5 mM $MgCl_2$, 0.2 mM EDTA) and homogenized briefly to break the nuclear membrane. An equal volume of high salt buffer (1.2 M KCl, 20 mM Tris, pH 7.3, 25% glycerol, 1.5 mM $MgCl_2$, 0.2 mM EDTA) was added followed by agitation for 30 min at 4 °C, and the samples were spun down at $20,000 \times g$ for 30 min. The supernatant was dialyzed in BC0 buffer (20 mM Tris, pH 7.3, 20% glycerol, 0.2 mM EDTA, 0.2 mM phenylmethylsulfonyl fluoride, and 10 mM 2-mercaptoethanol) for 3 h and centrifuged again. The cleared supernatant was then separated into aliquots, quickly frozen, and stored at −80 °C.

Immunoprecipitation and Mass Spectrometry—For large scale affinity purification, ~70 mg of nuclear protein extract was thawed gently and centrifuged at $100,000 \times g$ at 4 °C to spin down denatured protein. The supernatant was immunoprecipitated with 100 μl of M2 anti-FLAG-agarose beads (3.3 mg/ml, Sigma) for 3 h at 4 °C. The beads were then washed 4 times with NETN (20 mM Tris, pH 8.0, 100 mM NaCl, 0.5% Nonidet P-40, and 1 mM EDTA), and the bound protein was eluted twice with 100 μl of 200 μg/ml FLAG peptide (DYKDDDDK) (Sigma) in NETN. The eluant and bead fractions were boiled in SDS loading buffer, separated on a precast 8–12% SDS-PAGE gradient gel (Bio-Rad), and visualized by Coomassie Blue staining. Bands were excised, digested in trypsin and subjected to ion trap mass spectrometry as previously described (29). Peptides were identified using PROWL (prowl.rockefeller.edu).

For small scale immunoprecipitation experiments, 1–3 mg of nuclear extracts were incubated for 2 h at 4 °C with 5 μl of M2 anti-FLAG-agarose beads or 10 μg of anti-hRap1 antibody (Bethyl Laboratories) and 15 μl of protein A/G agarose beads. Ethidium bromide was added to a final concentration of 100 μg/ml. The beads were then washed four times with 0.5 ml NETN, boiled in SDS loading buffer, and separated on 8 or 10% SDS-PAGE gels.

Antibodies and Western Blotting Analysis—For Western analysis, immunoprecipitates and nuclear extract controls were separated by SDS-PAGE and transferred to polyvinylidene difluoride membranes. The primary antibodies mouse monoclonal anti-Rad50 (Gene Tex, MS-Rad 10-PX1), anti-FLAG M2 (Sigma, F-3165), mouse monoclonal anti-TRF2 (Oncogene, OP129–100UG), and goat anti-PARP1 (Santa Cruz Biotechnology, sc-1561). The secondary antibodies included anti-goat horseradish peroxidase (Santa Cruz, SC-2354), anti-mouse horseradish peroxidase (Bio-Rad, 170–6516), anti-rabbit horseradish peroxidase (Cell Signaling). The rabbit polyclonal anti-hRap1 antibody (Bethyl Laboratories) was generated against glutathione *S*-transferase-tagged full-length hRap1 fusion protein. The anti-hRap1 antibody was affinity-purified and shown to be able to Western blot, immunoprecipitate, and immuno-stain endogenous hRap1 (see Figs. 2–4).

Retroviral Small Hairpin Interference RNA (shRNA) Vector Construction and hRap1 Knockdown—The mouse U6 (mU6) RNA promoter (−315 bp) was PCR-amplified using mouse 32D cell genomic DNA as template. The mU6 promoter was then linked to EM7-Zeo (Zeocin resistance, Invitrogen) flanked by BamHI and HindIII sites to generate the mU6-Zeo cassette. EM7-Zeo was used as stuffer DNA to facilitate cloning. To construct a retroviral vector (pCL-puro-mU6) for expression of shRNA, the cytomegalovirus promoter was first cloned into the 5′ long terminal repeat of pBabe-puro. Then the BamH1 and HindIII sites on pCL-puro were destroyed before the mU6-Zeo cassette was cloned between the NheI and XbaI sites of the 3′ long terminal repeat region. For the hRAP1 shRNA vector, oligo 1 (GATCTTTgagagccctcctgattttgaaTTCAAGAGAttcaaaatcaggagggctctcTTTTTG-GA) and oligo 2 (AGCTTCCAAAAAgagagccctcctgattttgaaTCTCTTGAAttcaaaatcaggagggctctcA-AA) were annealed and ligated between the BamH1 and HindIII sites of pCL-puro-mU6.

Quantification of Telomere Length—HT1080 and HTC75 cells stably expressing hRap1 or shRNA constructs were passaged and harvested at different population doubling time points for DNA extraction (DNeasy Tissue Kit, Qiagen). Telomere restriction fragment length analysis was performed as described (2, 30) using restriction enzymes HinF1 and RSA1 (New England Biolabs) and the ^{32}P-labeled oligo probe $(TTAGGG)_3$. Quantification of telomere length was performed using ImageQuant software (Molecular Dynamics) and TELORUN (31).

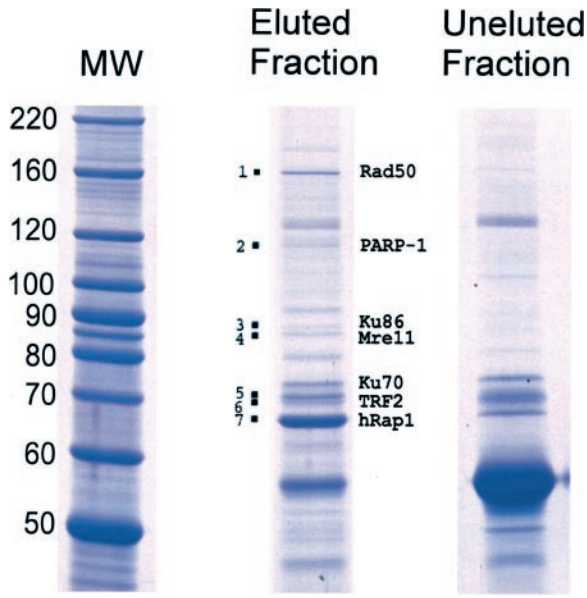

FIG. 1. **Analysis of the hRap1 complex by immunoprecipitation and mass spectrometry.** Nuclear extracts of HeLa S3 cells stably expressing FLAG-hRap1 were collected, immunoprecipitated with anti-FLAG conjugated agarose beads, and eluted with the FLAG peptide. The eluants were subsequently separated by SDS-PAGE, and the individual bands were identified by ion trap mass spectrometry.

Immunofluorescence—The localization of telomere-associated proteins was visualized through indirect immunofluorescence as previously described (7). Cells were grown overnight on coverslips, permeabilized in the Triton X-100 solution (0.5% Triton X-100 in phosphate-buffered saline), fixed with 3.7% paraformaldehyde in phosphate-buffered saline, and permeabilized again in the Triton X-100 solution containing 300 mM sucrose. The cells were subsequently blocked for 1 h at 37 °C in 5% goat serum, stained with various primary and fluorescence-conjugated secondary antibodies for 1 h each at 37 °C, and then visualized under a Nikon TE200 fluorescence microscope. Primary antibodies used are polyclonal anti-hRap1 antibody (Bethyl Laboratories), polyclonal anti-FLAG antibody (Sigma), and monoclonal anti-TRF2 antibody (Oncogene Science). Secondary antibodies are Alexfluo 488-conjugated goat anti-mouse antibody (Molecular Probes) and Texas Red goat anti-rabbit antibody (Rockland).

RESULTS

Identification of the hRap1 Protein Complex—To identify the hRap1 complex, an affinity purification method was utilized (see "Material and Methods"). HeLa S3 cells stably expressing FLAG-tagged hRap1 were first generated. Similar to endogenous hRap1, FLAG-hRap1 remained co-localized with endogenous TRF2 in these cells (see Fig. 5*B*), suggesting that FLAG-tagged hRap1 was targeted to the telomeres in the same fashion as endogenous hRap1 (7). Nuclear proteins were then extracted from these cells and immunoprecipitated with an anti-FLAG antibody that was conjugated to agarose beads. The precipitated proteins were eluted with FLAG peptides and separated by SDS-PAGE (Fig. 1). Distinct bands (compared with uneluted fractions) were subsequently excised, trypsin-digested, and sequenced by mass spectrometry.

We found hRap1 to co-purify with TRF2 (*band 6*) (Fig. 1 and Table I), in agreement with previous findings that hRap1 associates with TRF2 (7). In addition, Rad50 (*band 1*) and Mre11 (*band 4*) were detected. Both Rad50 and Mre11 are subunits of the MRN complex, which has been shown to interact with TRF2 (22). NBS1, the other subunit of the MRN complex, was not detected in our large scale immunoprecipitation experi-

TABLE I
Peptide sequences of the hRap1 complex identified by mass spectrometry

Band	Protein	Peptides
1	Rad50	QKFDEIFSATR
		YELQQLEGSSDR
2	PARP1	KPPLLNNADSVQAK
3	Ku86	HLMLPDFDLLEDIESK
4	Mre11	GNDTFVTLDEILR
		VDYSGGFEPFSVLR
5	Ku70	SDSFENPVLQQHFR
6	TRF2	DIMQALLVRPLGK
		DLVLPTQALPASPALK
		TLSGAQDSEAA
		WTVEESEWVK
7	hRap1	FNLDLSTVTQAFLK
		IAFTDADDVAILTYVK
		PGALAEGAAEPEPQR
		NSGELEATSAFLASGQR
		YLLGDAPVSPSSQK
		DDGSSMSFYVRPSPAK
		SSLTQHSWQSLKDR

ments of hRap1. NBS1 has been shown, however, to associate with TRF2 only in S-phase (22).

Interestingly, a number of proteins involved in DNA damage repair were also found to co-purify with hRap1. The p110 band (*band 2*) turned out to be poly(ADP-ribose) polymerase (PARP1) (32). Two other PARPs, namely tankyrase 1 and 2, interact with TRF1 and are known regulators of telomere length in mammalian cells (10, 33–36). Two additional DNA damage repair proteins found in the hRap1 complex are Ku86 and Ku70 (*bands 3* and *5*). These two proteins heterodimerize and are required for double-strand DNA break repair (37). Previous studies have found that Ku70 and Ku86 associate with telomeres (38–40). Our data suggest that the Ku70/86 heterodimer may be alternatively recruited to the telomeres through its interaction with the hRap1 complex.

Endogenous hRap1 Associates with Ku86 and Rad50—We next examined the interaction between endogenous hRap1 and the proteins identified in the hRap1 complex through immunoprecipitation experiments with anti-hRap1 and anti-TRF2 antibodies. Ethidium bromide was added in the reactions to rule out the possibility that some proteins might associate with hRap1 through double-stranded DNA. As shown in Fig. 2, immunoprecipitation of endogenous hRap1 from HeLa cell nuclear extracts was able to specifically pull down TRF2, Ku86, Rad50, and hRap1. Similarly, hRap1, Ku86, and Rad50 were also detected in the immunoprecipitates of endogenous TRF2. This result suggests that hRap1 as well as TRF2 interacts with Ku86 and the MRN complex *in vivo*.

Structural Organization of the hRap1 Protein Complex—To delineate how different regions of the hRap1 protein may interact with other proteins in the hRap1 complex, FLAG-tagged hRap1 deletion mutants lacking each of the four predicted domains or the linker region between the Myb and coil-coil domains were constructed (Fig. 3*A*). HeLa S3 cells that stably expressed these mutants were then generated. The expression levels of hRap1 mutants were about 1–5-fold of the endogenous protein (Fig. 3*D*). The different hRap1 mutant proteins were subsequently immunoprecipitated using the anti-FLAG antibody, and their associations with TRF2 and Rad50 were analyzed. As shown in Fig. 3*B*, hRap1 mutants lacking the RCT domain (ΔRCT) or both the coiled-coil and RCT domains (ΔRΔC) failed to immunoprecipitate TRF2. These results suggest that the hRap1 RCT domain mediates hRap1 association with TRF2 *in vivo*. This is consistent with previous findings that the hRap1 RCT domain could bind TRF2 through yeast-two-hybrid studies (7).

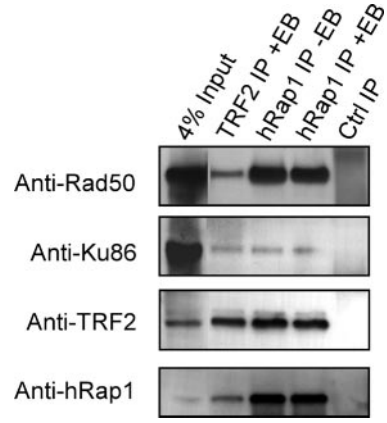

FIG. 2. **Endogenous hRap1 co-immunoprecipitated with proteins identified by mass spectrometry.** Endogenous hRap1 or TRF2 was immunoprecipitated using HeLa S3 cell nuclear extracts with a polyclonal antibody against hRap1 (*Rap1 IP*), a monoclonal antibody against TRF2 (*TRF2 IP*), or an anti-FLAG antibody (*Ctrl IP*). Immunoprecipitations were carried out in the presence (+) or absence (−) of 100 μg/ml ethidium bromide (*EB*). The precipitates were separated by SDS-PAGE, blotted, and probed with antibodies against hRap1, TRF2, Ku86, and Rad50.

We showed above that members of the MRN complex can associate with hRap1 *in vivo*. This interaction may occur through TRF2, as previously hypothesized (6). If this is the case, the hRap1 ΔRCT mutants that have lost the TRF2 binding abilities should fail to bind the MRN complex. To our surprise, both the ΔRCT and ΔRΔC hRap1 mutants still retained their binding activity with Rad50 and Mre11 (Fig. 3*B*). In fact, none of the mutations tested ablated or diminished the association of hRap1 with members of the MRN complex. Interestingly, Ku86 association was not abolished among the Rap1 mutants (Fig. 3*B*), albeit a reduction of Ku86 association was detected for two of the hRap1 mutants (ΔMyb and ΔBRCT). Because the interactions between hRap1 and Rad50/Mre11 or Ku86 were maintained even in mutants that failed to bind TRF2, it is therefore likely that hRap1 can recruit Rad50, Mre11, and Ku86 independent of TRF2. It also suggests that multiple domains of hRap1 may be involved in binding of these proteins.

We next examined the interaction of PARP1 with the various hRap1 mutants. In contrast to the proteins examined above, PARP1 no longer co-purified with the hRap1 ΔRCT mutant (Fig. 3*C*). This was not the case, however, for the hRap1 ΔMyb, ΔLink (Fig. 3*C*), and ΔBRCT mutants (data not shown). Therefore, PARP1 likely binds hRap1 either directly to the RCT domain or indirectly through TRF2.

hRap1 Negatively Regulates Telomere Length—Overexpression of full-length hRap1 was shown to extend telomeres in HT1080-derived HTC75 cells (7, 17). Whether endogenous hRap1 is a positive or negative regulator of telomere length, however, remains unknown. In addition, if hRap1 does regulate telomere length *in vivo*, which protein(s) may be necessary for such activity remains to be determined. To address the role of hRap1 in telomere length control, we first generated HTC75 cells in which hRap1 levels were stably reduced using shRNA (26, 27, 41). Western blot analyses indicated that endogenous hRap1 levels decreased significantly (50.0 ± 10.0%) in hRap1 shRNA cells (Fig. 4*A*). This inhibition of hRap1 expression was sustained for weeks, allowing for relatively long term studies of telomere length in these cells. We then compared the telomere length of these hRap1 knockdown cells to that of control cells at different cell passages. As shown in Fig. 4*B*, knockdown of hRap1 resulted in detectable extension of telomeres (~500 bp) as early as population doubling 10. This finding not only im-

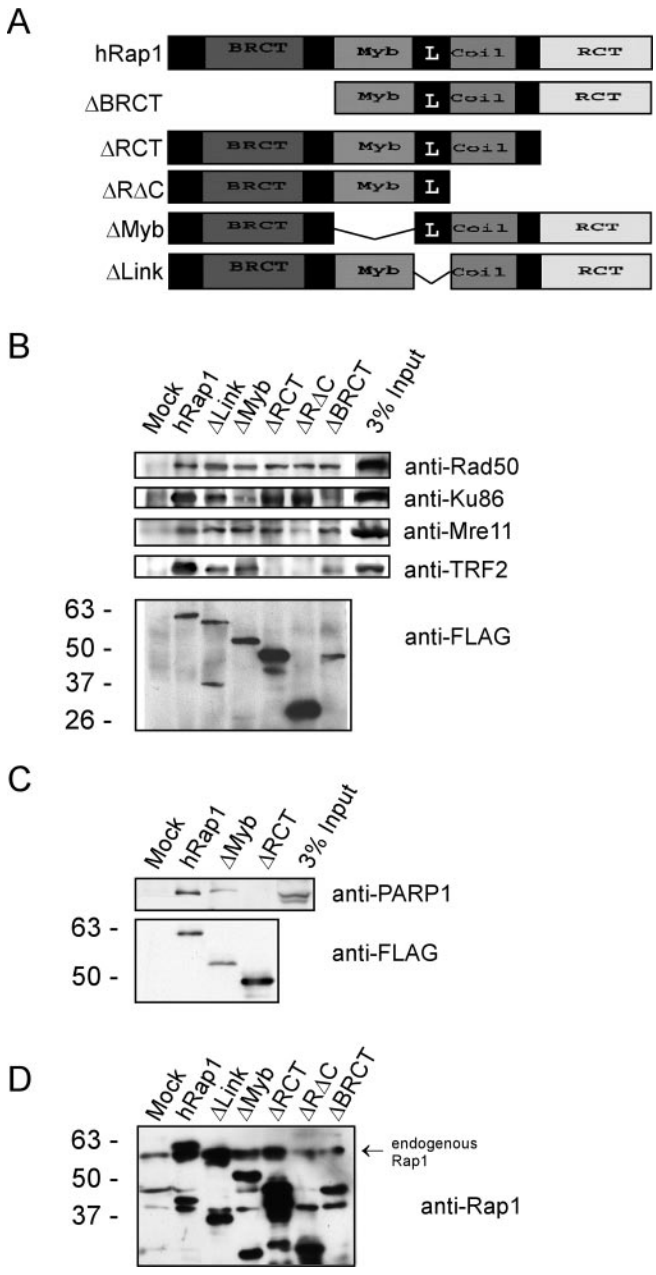

FIG. 3. **Deletional analysis of the interaction of the hRap1 complex.** *A*, a schematic representation of various hRap1 deletion mutant constructs. Each construct was FLAG-tagged (see "Materials and Methods" for details). *L* stands for the linker region. *B*, nuclear extracts of HeLa S3 cells stably expressing full-length and mutant hRap1 were collected. The nuclear extracts were then immunoprecipitated with an anti-FLAG antibody followed by SDS-PAGE and Western blotting with anti-Rad50, anti-Ku86, anti-TRF2, and anti-FLAG antibodies. *C*, similarly, FLAG-tagged hRap1 mutants were immunoprecipitated with an anti-FLAG antibody and blotted with anti-PARP1 and anti-FLAG antibodies. *D*, Western blot of endogenous and hRap1 mutant constructs. The blot was probed with a polyclonal antibody against hRap1, which recognizes both endogenous hRap1 and FLAG-tagged constructs (in *C*).

plicates hRap1 in negatively regulating telomere length but also suggests that this activity is evolutionarily conserved from yeast to human.

Telomeric Localization of hRap1 Mutants and Their Modulation of Telomere Length—We have thus far shown that hRap1 can bind TRF2, PARP1, Ku86, and the MRN complex. To determine which of these proteins may be responsible for hRap1 activity, we tested how the expression of hRap1 and various hRap1 mutant constructs (Fig. 3*A*) might influence hRap1 localization and telomere length. Both full-length and mutant hRap1 proteins were well expressed in the HT1080 cells. The subcellular localization of the various Rap1 proteins was then determined. Consistent with previous findings (7), endogenous hRap1 (*red*) exhibited a punctate pattern and co-stained with endogenous TRF2 (*green*) (Fig. 5A). Similar results were obtained in cells stably expressing the FLAG-tagged ΔBRCT mutant (Fig. 5*C*), indicating that the hRap1 ΔBRCT mutant can co-localize with endogenous TRF2. However, although the ΔRCT mutant also exhibited a punctate pattern, it did not co-stain with TRF2 (Fig. 5*D*). These observations support the model that the RCT domain is critical for hRap1 and TRF2 interaction and telomere association. Genomic DNA was extracted from these stable cells at different passages, and their telomere length was compared using the telomere restriction fragment assay.

Because the mutants differed in their localization and ability to bind TRF2, we expected to see differences in their effects on telomere length. Indeed, results from independent experiments indicated that the mutants extended telomere length to various degrees over generations (Fig. 6 and data not shown). Notably, the ΔBRCT mutant cells had consistently longer telomeres at late passages than other mutants. ΔBRCT telomere length was significantly longer than control (at PD70, $p = 0.049$). Full-length hRap1 overexpression also extended telomeres significantly (at PD70, $p = 0.012$). These results are in agreement with a recent report from Dr. de Lange's group (17). Because hRap1 RNA interference resulted in longer telomeres (Fig. 4), the hRap1 deletion mutants might function as dominant negatives to extend telomere length. Interestingly, the RCT deletion mutant (ΔRCT) had a much weaker telomere extension phenotype compared with full-length hRap1 (at PD70, 5.7 *versus* 7.2 kilobases, $p = 0.004$). Therefore, it suggests that the RCT domain may be necessary for the efficient inhibition of endogenous hRap1 function by overexpressed hRap1 mutants. Taken together with our immunoprecipitation results (Figs. 1–3), these data point to a model in which overexpression of hRap1 mutants might block proper telomeric access of signaling components that negatively regulate telomere length. In addition, the RCT-TRF2 interaction may be important for telomere length regulation of hRap1.

The Linker Region May Be Required for the Dominant Negative Effect of hRap1—The hRap1 mutants tested thus far all resulted in dominant negative phenotypes. Upon close examination, we found a small linker region situated between the Myb and coiled-coil domains that had been retained in all the mutants (Fig. 3*A*). We reasoned that this linker region might participate in recruiting the putative negative regulator(s). To test this possibility, we generated HT1080 cells expressing the hRap1 mutant with the linker region deleted (ΔLink) (Fig. 3*A*) and found this mutant to co-localize with TRF2 (Fig. 5*E*). In addition, binding of Rad50, Ku86, and TRF2 was not disrupted by the linker deletion (Fig. 3*B*). In contrast to full-length hRap1, however, expression of this mutant in HT1080 cells no longer lengthened telomeres (Fig. 6). This intriguing finding suggested that the linker domain of hRap1 might be necessary for hRap1 to negatively regulate telomere length. Because the ΔLink mutant still has an intact RCT domain and binds TRF2, its failure in telomere extension is likely caused by a mechanism other than RCT-TRF2 interaction. In an effort to understand the mechanism of the ΔLink affect on telomere length, we counted ΔLink and TRF2 foci in our immunofluoresence experiments. ΔLink co-localization with TRF2 was similar to that of full-length hRap1 (42 *versus* 41%). The slightly low level of total co-localization is likely due to and normally observed in

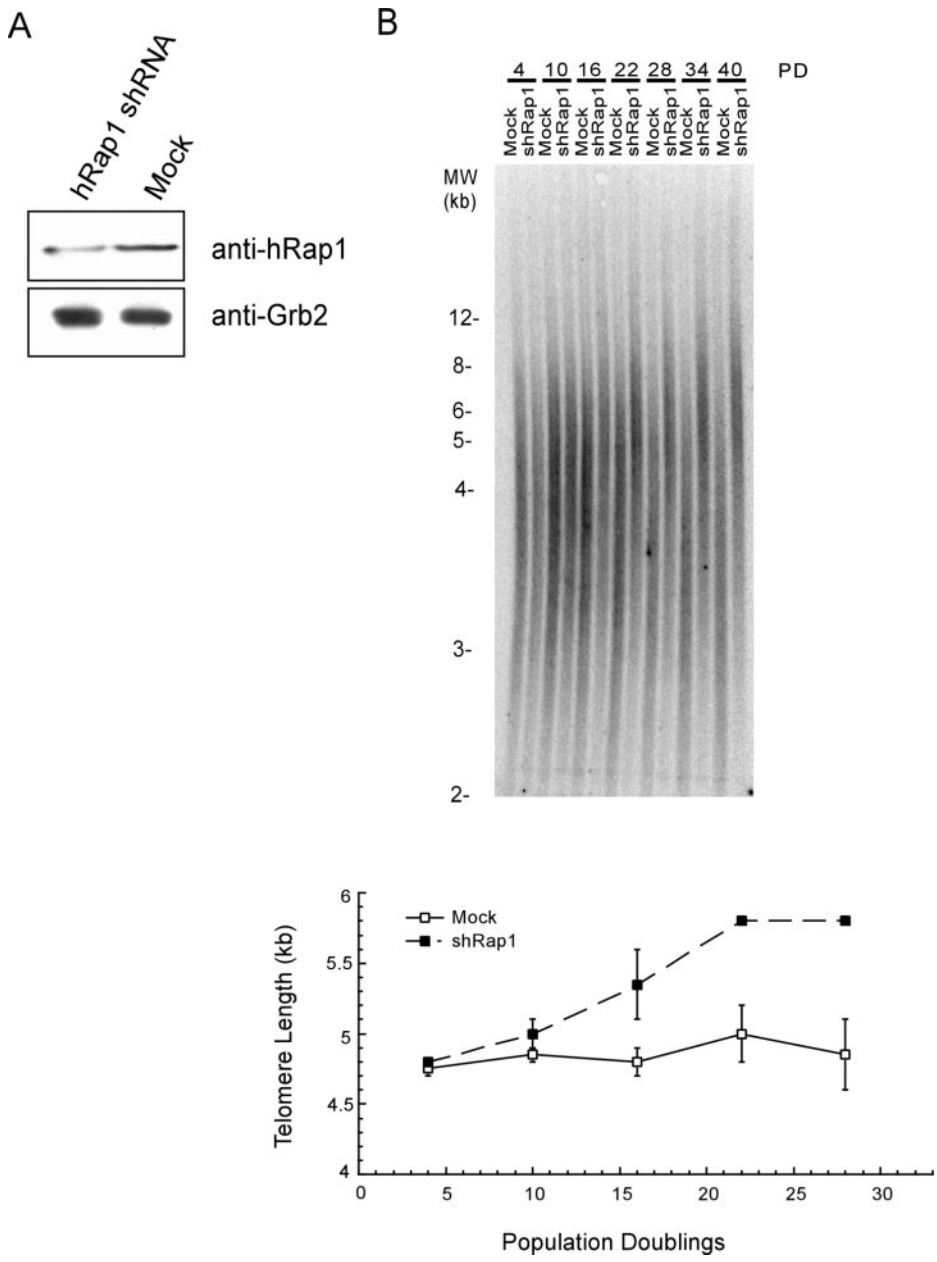

FIG. 4. **hRap1 negatively regulates telomere length.** *A*, endogenous hRap1 in HTC75 cells was knocked down with a retroviral vector encoding a shRNA against hRap1. A polyclonal anti-hRap1 antibody was used to Western blot for hRap1 expression. Densitometric analysis was performed to determine the difference in hRap1 expression (average knockdown was 50 ± 10% (S.E.)). An anti-GRB2 Western blot was used as loading control and for normalization. *B*, telomere restriction fragment length analysis of hRap1 knockdown cells. *Error bars* indicate the range of two different experiments. Mock and hRap1 shRNA cells were collected over generations. Non-telomeric genomic DNA was digested with HinF1 and RSA1, and the remaining telomeric DNA was separated on a 0.6% agarose gel and transferred to Nylon membranes. Southern blotting was performed, and the average size of telomeres was determined using ImageQuant software and TELORUN. *kb*, kilobases. *PD*, population doublings.

exogenously expressed protein. We did, however, detect a significant difference in the total number of observable TRF2 foci in ΔLink cells and full-length hRap1 cells (17.0 *versus* 22.8 foci per cell focus plane, $p < 0.0001$). This may reflect shorter telomere length in the ΔLink mutant cells. Alternatively, the ΔLink mutant may alter TRF2 telomere localization.

DISCUSSION

We have shown that hRap1 interacts with multiple proteins that are involved in DNA damage response pathways, including Rad50, Mre11, Ku70/86, and PARP1. Both the MRN and Ku70/86 complexes are known to regulate double-stranded DNA break repair and homologous recombination (42–44), whereas PARP1 modulates chromatin structure in response to stress (45). Although the exact role of these DNA-damage-response proteins at mammalian telomeres remains to be determined, genetic experiments in yeast and *Arabidopsis thaliana* have linked them to telomere length control (46–51). Recent studies also indicate that TRF2 is necessary to maintain telomere state and genome stability (4, 52). Thus, hRap1 together with TRF2 may function to recruit the DNA damage response proteins for telomere maintenance.

Our data suggest that hRap1 can associate with MRN and Ku70/86 independent of TRF2. It is important to note that none of our mutants abolished MRN or Ku70/86 interaction with hRap1. Therefore, the MRN and Ku complexes may interact with multiple domains of hRap1 (*e.g.* with both the RCT domain and the BRCT domain or the coiled-coil domain and the BRCT domain).

Our results also support the hypothesis that hRap1 has an evolutionarily conserved role in telomere length regulation; specifically, hRap1 is a negative regulator of telomere length because inhibition of hRap1 by RNA interference resulted in longer telomeres. These findings are in agreement with studies in yeast where null mutations of Rap1 and Taz1 (a TRF2 ortholog) resulted in aberrant telomere elongation (8, 15, 16).

We were particularly intrigued by the fact that full-length hRap1, and several of the hRap1 mutants we tested lengthened telomeres. It is likely that exogenously expressed hRap1 acts as a dominant negative. Expression of these mutant proteins may

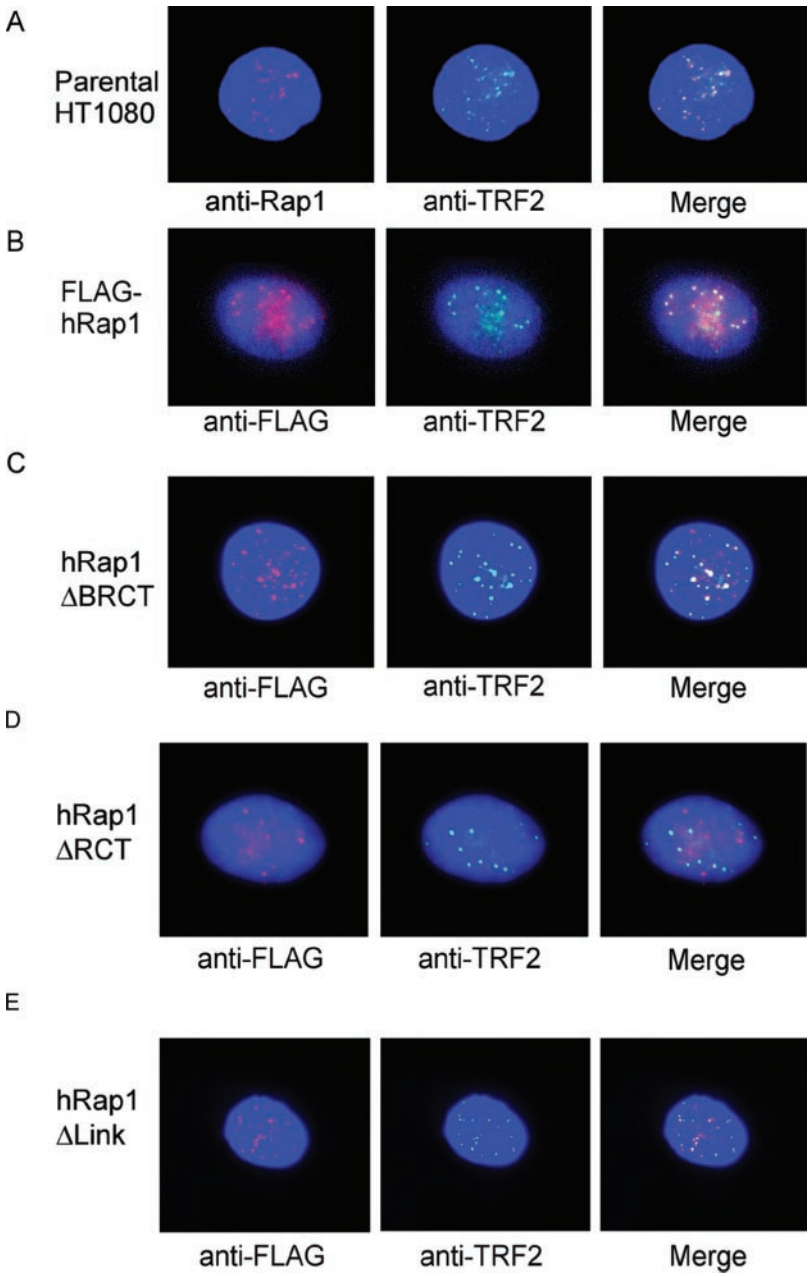

FIG. 5. **Telomeric localization of the hRap1 deletion mutants.** *A*, localization of endogenous hRap1. *B*, FLAG-hRap1. *C*, hRap1ΔBRCT. *D*, hRap1ΔRCT. *E*, hRap1ΔLink was examined by immunofluorescence with anti-hRap1 or anti-FLAG (*red*) and anti-TRF2 (*green*) antibodies. 4,6-Diamidino-2-phenylindole was used to visualize nuclear DNA (*blue*). *kb*, kilobases.

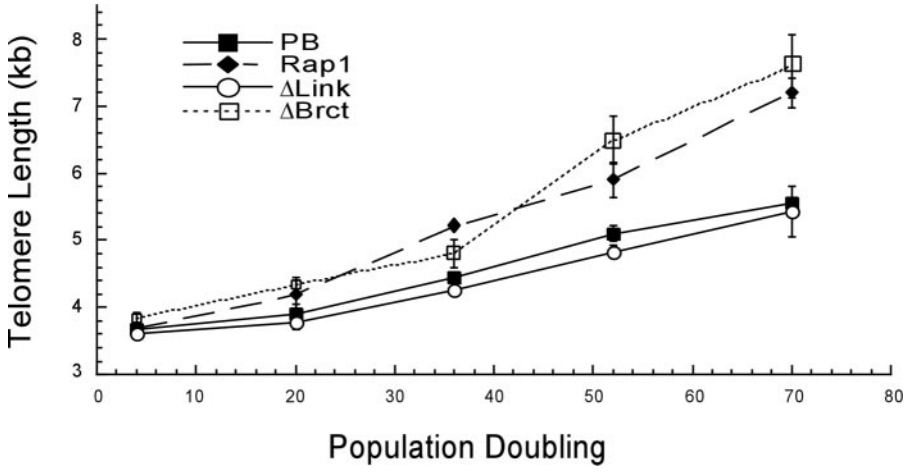

FIG. 6. **hRap1 mutants differentially affect telomere length.** Mock HT1080 cells and those expressing full-length hRap1, ΔBRCT, and ΔLink mutants were passaged over 70 generations, and their genomic DNA was collected for telomere restriction fragment length analysis to determine telomere length (see "Materials and Methods"). *Error bars* indicate S.E. from three different experiments. *PD*, population doublings.

prevent the association of protein(s) that normally controls telomere length with endogenous hRap1. TRF2 may play an important role in this process; for example, heterodimerization of TRF2 and hRap1 may be required for normal hRap1 function. The inability of the ΔRCT hRap1 mutants to greatly extend telomere length is likely due to the fact that they do not bind TRF2 and, therefore, titrate fewer factors away from the telomere. The hRap1 mutants that contain the RCT domain may be in such excess as to be competing for endogenous TRF2 binding. Our data that the RCT deletion mutant were not as potent as RCT-containing hRap1 mutants in telomere elongation supported this notion. Such a dominant negative titration model of hRap1 overexpression would suggest that the negative regulators of telomere length are segregated away from the telomeres.

Deletion analyses suggested that the linker region of hRap1 protein may modulate recruitment of putative regulators of telomere length, given that the ΔLink mutant lacking this region was incapable of extending telomeres. There is the possibility that deletion of the linker domain might have affected the folding of hRap1. However, the ΔLink protein expressed well, maintained its association with components of the hRap1 complex, and was targeted to the telomeres. The fact that the ΔLink mutant seems to reduce the number of TRF2 foci in cells suggests that, while it is able to interact with TRF2 (Fig. 3*B*), it may disrupt TRF2 interaction with the telomere, leading to reduction in average telomere length. It is also possible that the linker domain may be involved in or regulate the recruitment of unidentified negative regulators of telomere length.

Interestingly, deletion of the BRCT domain had a greater impact on telomere elongation than other mutants (17). BRCT domains are found in many of the proteins involved in DNA damage response pathways (53). Recently, we demonstrated that BRCT domains mediate phosphorylation-dependent protein-protein interactions (54). It is, therefore, also possible that hRap1 may recruit a regulator of telomere length through its BRCT domain.

What are the negative regulators recruited by hRap1? We showed here that the MRN and Ku70/86 complex associated with hRap1 directly or indirectly, suggesting that the MRN and Ku70/86 complex may be part of the hRap1 binding factor(s) that modulates telomere length in human cells. In further support of this model, the Ku70/86 complex has been shown to be involved in double-stranded DNA break repair and telomere length maintenance (47–51, 55). In yeast and *A. thaliana*, Ku mutants extended telomeres (48–50). Furthermore, the MRN complex can regulate telomere length in a Ku-dependent manner in *S. cerevisiae* (47). Ku70 and TRF2 have been reported to directly interact with each other through yeast two hybrid and *in vitro* binding experiments (39). Ku has also been proposed to be a direct regulator of human telomerase (56). hRap1/TRF2 may, therefore, indirectly regulate telomerase by either recruitment or regulation of Ku. A reduction of Ku86 association was detected for the ΔMyb and ΔBRCT Rap1 mutants, concurrent with the telomere-lengthening phenotype. However, we found that wild type hRap1 but not the ΔLink mutant extended telomeres yet still bound both Rad50 and Ku86. This implies that the Ku70/86 complex may not be the sole negative factors recruited by hRap1. It is possible that the linker domain may bind an unknown factor, which in turn regulates the activity of telomeric Ku70/86 complexes.

Acknowledgments—We thank Andy Laegeler for technical support and Dr. Titia de Lange for the HTC75 cell line.

REFERENCES

1. Broccoli, D., Smogorzewska, A., Chong, L., and de Lange, T. (1997) *Nat. Genet.* **17,** 231–235
2. Okabe, J., Eguchi, A., Masago, A., Hayakawa, T., and Nakanishi, M. (2000) *Hum. Mol. Genet* **9,** 2639–2650
3. de Lange, T. (2002) *Oncogene* **21,** 532–540
4. van Steensel, B., Smogorzewska, A., and de Lange, T. (1998) *Cell* **92,** 401–413
5. Blackburn, E. H. (2001) *Cell* **106,** 661–673
6. Kim Sh, S. H., Kaminker, P., and Campisi, J. (2002) *Oncogene* **21,** 503–511
7. Li, B., Oestreich, S., and de Lange, T. (2000) *Cell* **101,** 471–483
8. Krauskopf, A., and Blackburn, E. H. (1996) *Nature* **383,** 354–357
9. Shore, D. (1997) *Biol. Chem.* **378,** 591–597
10. Morse, R. H. (2000) *Trends Genet* **16,** 51–53
11. Grunstein, M. (1997) *Curr. Opin. Cell Biol.* **9,** 383–387
12. Gotta, M., and Cockell, M. (1997) *BioEssays* **19,** 367–370
13. Kyrion, G., Boakye, K. A., and Lustig, A. J. (1992) *Mol. Cell. Biol.* **12,** 5159–5173
14. Kyrion, G., Liu, K., Liu, C., and Lustig, A. J. (1993) *Genes Dev.* **7,** 1146–1159
15. Kanoh, J., and Ishikawa, F. (2001) *Curr. Biol.* **11,** 1624–1630
16. Park, M. J., Jang, Y. K., Choi, E. S., Kim, H. S., and Park, S. D. (2002) *Mol. Cell* **13,** 327–333
17. Li, B., and De Lange, T. (2003) *Mol. Biol. Cell* **14,** 5060–5068
18. Konig, P., Giraldo, R., Chapman, L., and Rhodes, D. (1996) *Cell* **85,** 125–136
19. Longtine, M. S., Wilson, N. M., Petracek, M. E., and Berman, J. (1989) *Curr. Genet.* **16,** 225–239
20. Moretti, P., Freeman, K., Coodly, L., and Shore, D. (1994) *Genes Dev.* **8,** 2257–2269
21. Hanaoka, S., Nagadoi, A., Yoshimura, S., Aimoto, S., Li, B., de Lange, T., and Nishimura, Y. (2001) *J. Mol. Biol.* **312,** 167–175
22. Zhu, X. D., Kuster, B., Mann, M., Petrini, J. H., and de Lange, T. (2000) *Nat. Genet.* **25,** 347–352
23. Trujillo, K. M., and Sung, P. (2001) *J. Biol. Chem.* **276,** 35458–35464
24. Diede, S. J., and Gottschling, D. E. (2001) *Curr. Biol.* **11,** 1336–1340
25. Tsukamoto, Y., Taggart, A. K., and Zakian, V. A. (2001) *Curr. Biol.* **11,** 1328–1335
26. Hannon, G. J. (2002) *Nature* **418,** 244–251
27. Tuschl, T. (2001) *Chembiochem* **2,** 239–245
28. Pear, W. S., Nolan, G. P., Scott, M. L., and Baltimore, D. (1993) *Proc. Natl. Acad. Sci. U. S. A.* **90,** 8392–8396
29. Ogryzko, V. V., Kotani, T., Zhang, X., Schiltz, R. L., Howard, T., Yang, X. J., Howard, B. H., Qin, J., and Nakatani, Y. (1998) *Cell* **94,** 35–44
30. van Steensel, B., and de Lange, T. (1997) *Nature* **385,** 740–743
31. Ouellette, M. M., Liao, M., Herbert, B. S., Johnson, M., Holt, S. E., Liss, H. S., Shay, J. W., and Wright, W. E. (2000) *J. Biol. Chem.* **275,** 10072–10076
32. Ziegler, M., and Oei, S. L. (2001) *BioEssays* **23,** 543–548
33. Smith, S., Giriat, I., Schmitt, A., and de Lange, T. (1998) *Science* **282,** 1484–1487
34. Rippmann, J. F., Damm, K., and Schnapp, A. (2002) *J. Mol. Biol.* **323,** 217–224
35. Seimiya, H., and Smith, S. (2002) *J. Biol. Chem.* **277,** 14116–14126
36. Sbodio, J. I., Lodish, H. F., and Chi, N. W. (2002) *Biochem. J.* **361,** 451–459
37. Featherstone, C., and Jackson, S. P. (1999) *Curr. Biol.* **9,** 759–761
38. Hsu, H. L., Gilley, D., Blackburn, E. H., and Chen, D. J. (1999) *Proc. Natl. Acad. Sci. U. S. A.* **96,** 12454–12458
39. Song, K., Jung, D., Jung, Y., Lee, S. G., and Lee, I. (2000) *FEBS Lett.* **481,** 81–85
40. Samper, E., Goytisolo, F. A., Slijepcevic, P., van Buul, P. P., and Blasco, M. A. (2000) *EMBO Rep.* **1,** 244–252
41. Elbashir, S. M., Harborth, J., Lendeckel, W., Yalcin, A., Weber, K., and Tuschl, T. (2001) *Nature* **411,** 494–498
42. Connelly, J. C., and Leach, D. R. (2002) *Trends Biochem. Sci.* **27,** 410–418
43. Hopfner, K. P., Putnam, C. D., and Tainer, J. A. (2002) *Curr. Opin. Struct. Biol.* **12,** 115–122
44. Sung, P., Trujillo, K. M., and Van Komen, S. (2000) *Mutat. Res.* **451,** 257–275
45. Smith, S. (2001) *Trends Biochem. Sci.* **26,** 174–179
46. Nugent, C. I., Bosco, G., Ross, L. O., Evans, S. K., Salinger, A. P., Moore, J. K., Haber, J. E., and Lundblad, V. (1998) *Curr. Biol.* **8,** 657–660
47. Boulton, S. J., and Jackson, S. P. (1998) *EMBO J.* **17,** 1819–1828
48. Gallego, M. E., Jalut, N., and White, C. I. (2003) *Plant Cell* **15,** 782–789
49. Bundock, P., van Attikum, H., and Hooykaas, P. (2002) *Nucleic Acids Res.* **30,** 3395–3400
50. Riha, K., Watson, J. M., Parkey, J., and Shippen, D. E. (2002) *EMBO J.* **21,** 2819–2826
51. Driller, L., Wellinger, R. J., Larrivee, M., Kremmer, E., Jaklin, S., and Feldmann, H. M. (2000) *J. Biol. Chem.* **275,** 24921–24927
52. Karlseder, J., Smogorzewska, A., and de Lange, T. (2002) *Science* **295,** 2446–2449
53. Bork, P., Hofmann, K., Bucher, P., Neuwald, A. F., Altschul, S. F., and Koonin, E. V. (1997) *FASEB J.* **11,** 68–76
54. Rodriguez, M., Yu, X., Chen, J., and Songyang, Z. (2003) *J. Biol. Chem.* **278,** 52914–52918
55. Bailey, S. M., Meyne, J., Chen, D. J., Kurimasa, A., Li, G. C., Lehnert, B. E., and Goodwin, E. H. (1999) *Proc. Natl. Acad. Sci. U. S. A.* **96,** 14899–14904
56. Chai, W., Ford, L. P., Lenertz, L., Wright, W. E., and Shay, J. W. (2002) *J. Biol. Chem.* **277,** 47242–47247

THE JOURNAL OF BIOLOGICAL CHEMISTRY
Vol. 279, No. 49, Issue of December 3, pp. 51338–51342, 2004
Printed in U.S.A.

Telosome, a Mammalian Telomere-associated Complex Formed by Multiple Telomeric Proteins*

Received for publication, August 13, 2004, and in revised form, September 20, 2004
Published, JBC Papers in Press, September 20, 2004, DOI 10.1074/jbc.M409293200

Dan Liu‡§, Matthew S. O'Connor‡, Jun Qin, and Zhou Songyang¶

From the Verna and Marrs McLean Department of Biochemistry and Molecular Biology, Baylor College of Medicine, Houston, Texas 77030

In mammalian cells, telomere-binding proteins TRF1 and TRF2 play crucial roles in telomere biology. They interact with several other telomere regulators including TIN2, PTOP, POT1, and RAP1 to ensure proper maintenance of telomeres. TRF1 and TRF2 are believed to exert distinct functions. TRF1 forms a complex with TIN2, PTOP, and POT1 and regulates telomere length, whereas TRF2 mediates t-loop formation and end protection. However, whether cross-talk occurs between the TRF1 and TRF2 complexes and how the signals from these complexes are integrated for telomere maintenance remain to be elucidated. Through gel filtration and co-immunoprecipitation experiments, we found that TRF1 and TRF2 are in fact subunits of a telomere-associated high molecular weight complex (telosome) that also contains POT1, PTOP, RAP1, and TIN2. We demonstrated that the TRF1-interacting protein TIN2 binds TRF2 directly and *in vivo*, thereby bridging TRF2 to TRF1. Consistent with this multi-protein telosome model, stripping TRF1 off the telomeres by expressing tankyrase reduced telomere recruitment of not only TIN2 but also TRF2. These results help to unify previous observations and suggest that telomere maintenance depends on the multi-subunit telosome.

The homeostasis of mammalian telomeres is regulated by a number of telomere-associated proteins. Among these proteins, TRF1 and TRF2 directly bind double-stranded telomere DNA and interact with a number of proteins to maintain telomere length and structure (1, 2). It has been shown that the amount of telomere-bound TRF1 correlates with telomere length. Overexpression of TRF1 shortened telomeres in human cells, whereas dominant negative TRF1 led to elongated telomeres (3–5). TRF1 may control the length of telomere repeats through multiple mechanisms. For example, TRF1 can control telomerase access through its interaction with TIN2, PTOP/PIP1, and the single-stranded telomere DNA-binding protein POT1 (6–8). TRF1 may also regulate telomerase activity through its interaction with PINX1 (9). In comparison, TRF2 has an essential role in telomere end protection and t-loop formation (1, 10, 11). Interference of endogenous TRF2 activity by expressing dominant negative forms of TRF2 markedly increased the rate of telomere end-to-end fusions (12). Consistent with this role of TRF2, TRF2 forms a complex with RAP1 and associates with several proteins involved in DNA damage and repair responses, notably RAD50/MER11/NBS1, Ku86, and ERCC1/XPF (13–15). These findings have pointed to distinct biological functions of TRF1 and TRF2. Some recent findings, however, suggest a more complex picture. For instance, overexpression of TRF2 caused telomere shortening in primary cells (16). In mouse embryonic stem cells, the conditional knockout of TRF1 led to significantly reduced levels of TRF2 at the telomeres, suggesting that TRF2 telomere localization may be partially regulated by TRF1 (17). In addition, chromosome end-to-end fusion was detected in TRF1 knock-out cells, indicating that telomere end protection was compromised. Despite the wealth of information, the functional relationship between TRF1 and TRF2 in telomere maintenance remains unclear. Notably, a recent report demonstrated a direct interaction between TRF2 and the TRF1-interacting protein, TIN2 (18). Such findings further suggest that cross-talk probably occurs between the TRF1 and TRF2 complexes. However, whether TIN2 can simultaneously associate with both TRF1 and TRF2 in the same complex remains to be demonstrated.

In addition to TRF1, several other telomeric proteins have been shown to be regulators of telomere length (1, 2, 7, 8, 19–22). Both inhibition of endogenous RAP1, TIN2, POT1, or PTOP expression through RNA interference (RNAi)[1] and expression of dominant negative forms of these four proteins resulted in elongated telomeres in cultured cells (3, 6–8, 15, 23). These observations suggest that RAP1, TIN2, POT1, and PTOP may function in the same pathway. All four proteins, RAP1, TIN2, POT1, and PTOP, directly or indirectly associate with TRF1 or TRF2 (7, 8, 20), pointing to a possible functional connection among these six telomeric proteins. In this report, we present evidence demonstrating that the TRF1 and TRF2 complexes do indeed interact with each other, as TRF1, TRF2, RAP1, TIN2, POT1, and PTOP can form a protein complex *in vivo* to regulate telomeres.

MATERIALS AND METHODS

Preparation of Nuclear Extracts—HeLa S3 cells grown in suspension to 1×10^6 cells/ml were collected and washed in cold phosphate-buffered saline and hypotonic buffer (10 mM Tris, pH 7.3, 10 mM KCl, 1.5 mM $MgCl_2$, 0.2 mM phenylmethylsulfonyl fluoride, and 10 mM 2-mercaptoethanol). The cells were then allowed to swell for 15 min in hypotonic buffer, homogenized until cell membrane lysis was ~80%. The lysates were resuspended in low salt buffer (20 mM KCl, 20 mM Tris, pH 7.3, 25% glycerol, 1.5 mM $MgCl_2$, and 0.2 mM EDTA) and homogenized briefly to break the nuclear membrane. An equal volume

* This work was supported by grants from the Department of Defense and the National Institute of Health (to Z. S.). The costs of publication of this article were defrayed in part by the payment of page charges. This article must therefore be hereby marked "*advertisement*" in accordance with 18 U.S.C. Section 1734 solely to indicate this fact.

‡ Both authors contributed equally to this work.

§ To whom correspondence may be addressed. E-mail: danl@bcm.tmc.edu.

¶ To whom correspondence may be addressed: Dept. of Biochemistry and Molecular Biology, Baylor College of Medicine, One Baylor Plaza, Houston, TX 77030. E-mail: songyang@bcm.tmc.edu.

[1] The abbreviations used are: RNAi, RNA interference; TANK, tankyrase; GST, glutathione *S*-transferase; PD, poly(ADP-ribose) polymerase-dead.

of high salt buffer (1.2 M KCl, 20 mM Tris, pH 7.3, 25% glycerol, 1.5 mM $MgCl_2$, and 0.2 mM EDTA) was added followed by agitation for 30 min at 4 °C and centrifuged at 20,000 × *g* for 30 min. The supernatant was dialyzed in BC0 buffer (20 mM Tris, pH 7.3, 20% glycerol, 0.2 mM EDTA, 0.2 mM phenylmethylsulfonyl fluoride, and 10 mM 2-mercaptoethanol) for 3 h and centrifuged again. The cleared supernatant was then aliquoted and stored at −80 °C.

Salt extraction and fractionation of HT1080 cells were performed as previously described previously (23). The cells were extracted in a low salt buffer (20 mM Hepes pH 7.9, 5 mM $MgCl_2$, 1 mM DTT, 25% glycerol, protease inhibitors, 0.2% Nonidet P-40, and 150 mM KCl). The resulting supernatant was the 150 mM fraction. The pellet was further extracted with a similar buffer but containing 420 mM KCl. Chromatin-bound proteins were in the 420 mM KCl fraction.

Immunoprecipitation and Mass Spectrometry—For large-scale affinity purification, ~70 mg of nuclear protein extracts were incubated with 100 μl of anti-FLAG M2-agarose beads (Sigma) for 3 h at 4 °C. The beads were then washed 4 times with NETN (20 mM Tris, pH 8.0, 100 mM NaCl, 0.5% Nonidet P-40, and 1 mM EDTA), and the bound protein was eluted twice with 100 μl of 200 μg/ml FLAG peptide-(DYKDDDDK) (Sigma) in NETN. The eluent was resolved on a 8–12% SDS-PAGE gradient gel (Bio-Rad) and visualized by Coomassie Blue staining. Specific bands were then excised, digested with trypsin, and subjected to ion-trap mass spectrometry as previously described (24). Peptides were identified using PROWL (prowl.rockefeller.edu/).

For small-scale immunoprecipitation experiments, 1 mg of nuclear extracts was incubated for 2 h at 4 °C with 5 μg of anti-FLAG M2 (Sigma), anti-hRap1 (Bethyl Laboratories), anti-TRF2 (Oncogene), anti-POT1N, anti-TIN2C, or anti-PTOP 466 antibodies (7) and 15 μl of protein A or protein G-agarose beads (Santa Cruz Biotechnology). The beads were then washed four times with 0.5 ml of NETN, boiled in 2× SDS loading buffer, and resolved on 8 or 10% SDS-PAGE gels.

Fractionation of the Telomere-associated Complex, Telosome—Chromatographic experiments were performed as described previously (7). HeLa cell nuclear extracts were fractionated on ΔKTA Superose 6 HR 10/30 gel filtration columns (Amersham Biosciences). The resulting fractions were resolved by SDS-PAGE and probed with various antibodies.

Generation of Constructs and Cell Lines of hRap1 and Its Deletion Mutants—FLAG-tagged full-length hRap1 and various hRap1 mutants were cloned in the pBabe-puro retroviral vector as previously described (15). The retroviral wild type and mutant FLAG-tankyrase (TANK) vectors were a generous gift from Dr. Titia de Lange (23). The retroviral vectors were used to transfect BOSC23 cells to produce retroviruses for the subsequent infection of HeLa or HT1080 cells. These cells were selected with 2 μg/ml puromycin for 3 days after infection to obtain cells stably expressing hRap1 and its mutants or TANK.

Antibodies and Western Blotting Analysis—For Western analysis, immunoprecipitates and nuclear extract controls were separated by SDS-PAGE and transferred to polyvinylidene difluoride membranes. The primary antibodies included anti-FLAG M2 (Sigma) and anti-TRF2 (Oncogene). The rabbit polyclonal anti-POT1N antibody was generated against GST-tagged human POT1 protein (amino acids 1–253). Anti-RAP1, anti-TIN2C, and anti-PTOP 466 antibodies were previously described (7). These antibodies were generated by the Bethyl Laboratories. Anti-TRF1 antibody was a generous gift from the de Lange laboratory (3). The secondary antibodies included anti-mouse horseradish peroxidase and anti-rabbit horseradish peroxidase (Bio-Rad).

In Vitro Binding Assays—Bacterially expressed GST full-length POT1, RAP1, and TIN2 were purified using glutathione-agarose beads (Molecular Probes). Approximately 1 μg of GST fusion proteins on beads was used for each binding reaction. *In vitro* translation and [^{35}S]Met labeling of human TRF1 and TRF2 were carried out using the In Vitro TnT kit (Promega). The mixtures were washed three times with NETN, eluted with 2× SDS buffer, resolved by SDS-PAGE, and transferred to polyvinylidene difluoride membranes followed by analysis using a PhosphorImager (Amersham Biosciences).

Indirect Immunofluorescence—The localization of telomere-associated proteins were visualized through indirect immunofluorescence as previously described (20). Cells were grown overnight on poly-D-lysine-coated coverslips, permeabilized in the Triton X-100 solution (0.5% Triton X-100 in phosphate-buffered saline), fixed with 3.7% paraformaldehyde in phosphate-buffered saline, and permeabilized again in the Triton X-100 solution containing 300 mM sucrose. The cells were subsequently blocked for 1 h at 37 °C in 5% goat serum, stained with various primary and fluorescence-conjugated secondary antibodies for 1 h each at 37 °C, and then visualized under a Nikon TE200 fluorescence microscope. The primary antibodies used were: polyclonal anti-TRF1; anti-TIN2C antibody; and monoclonal anti-TRF2 antibody (Oncogene). Secondary antibodies were AlexaFluor 488-conjugated goat anti-mouse antibody (Molecular Probes) and Texas Red goat anti-rabbit antibody (Molecular Probes).

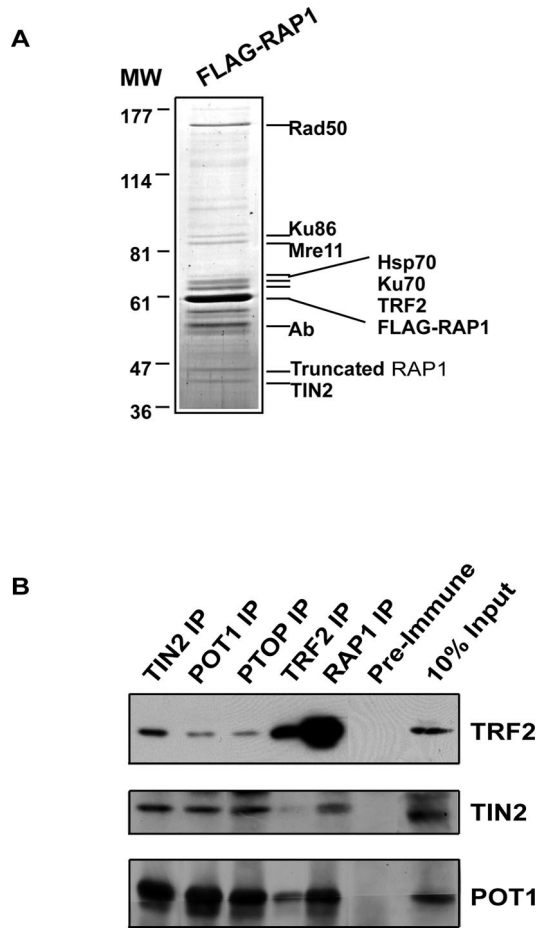

FIG. 1. **Association of TRF2·RAP1 with components of the TRF1 complex.** *A*, nuclear extracts from HeLa cells expressing FLAG-RAP1 were immunoprecipitated with anti-FLAG antibodies and resolved by SDS-PAGE. Specific bands were excised and sequenced by mass spectrometry. *MW*, molecular weight; *Ab*, antibody heavy chain. *B*, HeLa nuclear extracts were immunoprecipitated with anti-TIN2, anti-POT1, anti-PTOP, anti-TRF2, or anti-RAP1 antibodies. The immunoprecipitates were resolved by SDS-PAGE and Western blotted with the indicated antibodies. *IP*, immunoprecipitation. (Note: we could not Western blot PTOP or TRF1 in these co-immunoprecipitation experiments, because PTOP and TRF1 migrate to almost exactly the same location as antibodies.)

RESULTS

Identification of a Telomere-associated Protein Complex, Telosome—Individual proteins can be epitope-tagged, which allows for easy isolation and identification of their associated proteins by immunoprecipitation and mass spectrometry. We undertook such a proteomic approach to understand the molecular mechanisms that regulate human telomeres. In our analysis of the purified RAP1 protein complex, we identified several proteins that are known to interact with RAP1, including RAD50, Mre11, Ku86/70, and TRF2 (Fig. 1*A*) (13, 15). Intriguingly, the sequencing of the 40-kDa band revealed TIN2 as a component of the RAP1 complex as well. The same RAP1 complex was able to form even in the presence of ethidium bromide, suggesting that the interactions between the various components were not mediated through DNA (data not shown). The presence of TIN2 in the RAP1·TRF2 complex was surprising, because TIN2 is a TRF1-interacting protein (19).

Our purification and characterization of TIN2-associated proteins further confirmed the existence of a RAP1·TIN2 pro-

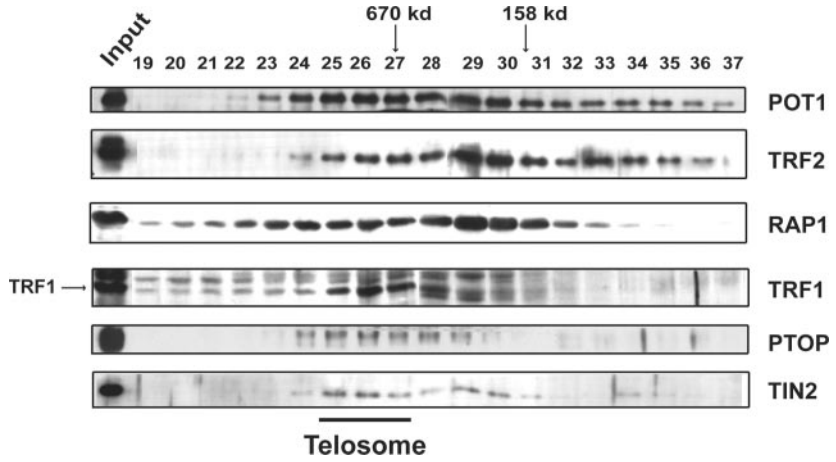

FIG. 2. **The six-telomeric proteins form a high molecular weight protein complex, the telosome.** HeLa S3 cell nuclear extracts were fractionated on a Superose 6 gel filtration column. Individual fractions (*numbered*) were collected, resolved by SDS-PAGE, and Western blotted with the indicated antibodies. Gel filtration molecular standards are indicated by *arrows*.

tein complex, as we found TRF2 and RAP1 to co-purify with TRF1, TIN2, PTOP, and POT1 (7). Furthermore, mass spectrometry sequencing revealed the six proteins to be the major components of the isolated complex (7). Because TIN2, PTOP, and POT1 have been shown to complex with TRF1 (6–8), it suggests that TRF2 and RAP1 may interact with the TRF1 complex, resulting in the formation of a six-protein complex at the telomeres.

To determine the interaction between the six telomeric proteins, we carried out co-immunoprecipitation experiments using nuclear extracts from HeLa cells and antibodies against endogenous POT1, PTOP, TIN2, RAP1, or TRF2. Consistent with our previous observations (7), endogenous POT1 and PTOP co-immunoprecipitated with TIN2, whereas immunoprecipitation with anti-PTOP and anti-TIN2 antibodies brought down POT1 (Fig. 1*B*). Notably, TRF2 was also able to co-immunoprecipitate with POT1, PTOP, and TIN2. In the reciprocal experiment, antibodies against TRF2 or RAP1 brought down POT1 and TIN2 as well. These data strongly support our findings that TRF2 and RAP1 associate with the TRF1 complex and suggest a cross-talk between the TRF1 and TRF2 complexes.

We performed gel filtration experiments next using HeLa nuclear extracts. As shown in Fig. 2, endogenous TRF1, TRF2, TIN2, RAP1, PTOP, and POT1 co-eluted in a large molecular complex (~1 MDa), indicating that the six-telomeric proteins could indeed form a physical complex that contains the major telomeric proteins identified to date in mammalian cells. Based on the above data, we named this large complex, containing the six telomeric proteins, the telosome. It should be noted that some of the telomeric proteins (*e.g.* RAP1 and TRF2) were also co-eluted at lower molecular weight fractions. Therefore, there may be other telomere complexes in addition to the telosome.

TIN2 Directly Binds TRF2 Both in Vitro and in Vivo and Tethers TRF2 to the TRF1 Complex—We next examined how the TRF2·RAP1 subcomplex was connected to the TRF1 subcomplex in the telosome. RAP1 contains an N-terminal BRCA1 C-terminal domain, a Myb domain, and a C-terminal TRF2-binding RAP1 C-terminal domain (RCT) (20). We first set out to determine which of the domains of RAP1 were necessary for its association with TIN2. As shown in Fig. 1*A*, anti-FLAG immunoprecipitation of full-length RAP1 brought down endogenous TRF2 and TIN2. An analysis of a series of RAP1 deletion mutants available in the laboratory (15) revealed that the BRCA1 C-terminal and Myb domains were dispensable in mediating RAP1 interaction with TRF2 and TIN2 (Fig. 3*A*). However, the RAP1 C-terminal domain deletion mutant (ΔRCT) failed to co-immunoprecipitate with not only endogenous TRF2 but also TIN2, indicating that RAP1 may associate with TIN2 through TRF2. Furthermore, these data suggest a direct interaction between TRF2 and TIN2 (or other components of the TRF1 complex). To test this hypothesis, TRF2 was *in vitro* translated and incubated with GST fusion telomeric proteins. As shown in Fig. 3*B*, *in vitro* translated TRF2 specifically bound GST-TIN2 (at a level comparable to GST-RAP1) but not GST-POT1. GST-TIN2 but not GST-RAP1 specifically pulled down *in vitro* translated TRF1 (Fig. 3*B*, *right panel*). Therefore, both TRF1 and TRF2 can directly interact with TIN2. Moreover, specific interactions between V5-tagged TRF2 and FLAG-tagged TIN2 were detected in 293T cells (data not shown). Consistent with a recent report on TIN2 interaction with TRF2 (18), our results indicate that TIN2 provides the link between the TRF1 and TRF2 complexes.

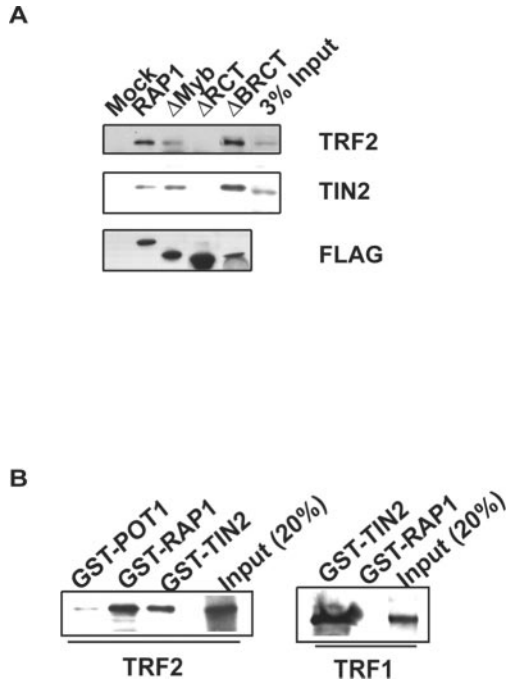

FIG. 3. **TIN2 directly interacts with TRF2.** *A*, extracts from cells expressing FLAG-tagged full-length RAP1, RAP1 ΔBRCT, RAP1 ΔMyb, and RAP1 ΔRCT were immunoprecipitated with anti-FLAG antibodies. The immunoprecipitates were resolved on SDS-PAGE and Western blotted using anti-TRF2 and anti-TIN2 antibodies. *B*, cDNAs encoding full-length TRF2 or TRF1 were cloned into the pcDNA3 vector and *in vitro* translated in the presence of [^{35}S]Met. GST-POT1, GST-TIN2, and GST-RAP1 fusion proteins were used in pull-down reactions.

Telomeric Localization of Telosome Subunits Is Regulated by TRF1—To further address the functional relevance of telosome as well as the interaction between TRF1 and TRF2, we inves-

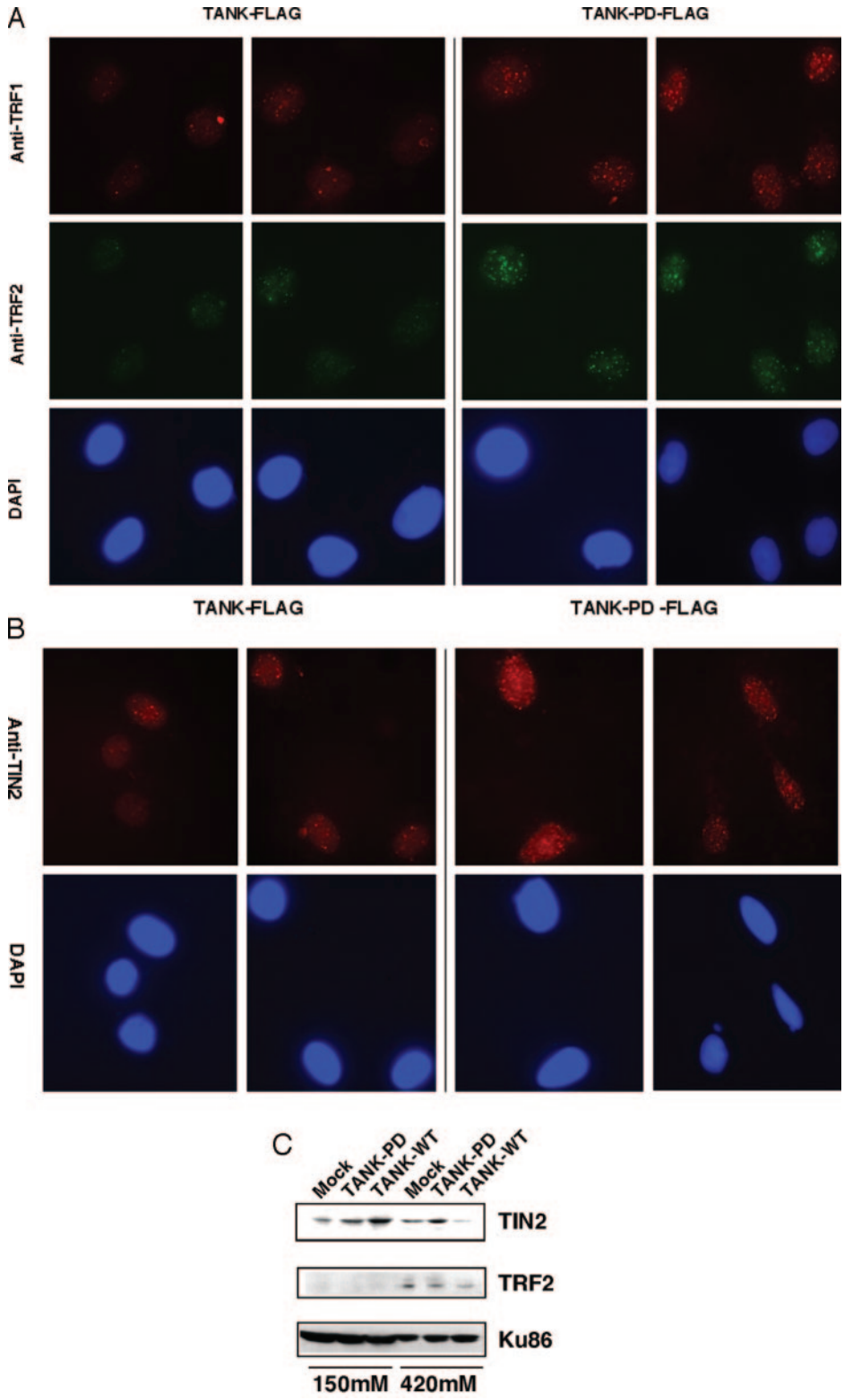

FIG. 4. **Telomeric localization of telosome subunits is regulated by TRF1.** HT1080 cells expressing wild type TANK (*two left panels*) or its catalytically inactive mutant (TANK-PD, *two right panels*) were twice permeabilized and stained with antibodies against TRF1, TRF2 (*A*), or TIN2 (*B*). *C*, HT1080 cells expressing TANK wild type or TANK-PD were extracted sequentially with buffer containing 150 and 420 mM KCl (chromatin-bound fraction) (23). The cell extracts were then Western blotted with anti-TIN2, anti-TRF2, and anti-Ku86 (loading control) antibodies.

tigated whether telomere localization of telosome subunits, in particular TRF2, was regulated by TRF1 using HT1080 cells expressing FLAG-tagged wild type TANK or catalytically inactive TANK (TANK-PD). TANK is a TRF1-associated poly(ADP-ribose) polymerase (25). TANK can ADP-ribosylate TRF1, resulting in TRF1 ubiquitination and degradation by the proteasome pathway, effectively stripping TRF1 off the telomeres (25, 26). In these cells, FLAG-TANK and TANK-PD were expressed at comparable levels, whereas total TIN2 and TRF2 levels were not reduced (data not shown). We then compared the levels of telomere-localized TRF1, TRF2, and TIN2 in these cells using indirect immunofluorescence. Endogenous TRF1, TRF2, and TIN2 exhibited punctate staining patterns, characteristic of telomeric proteins (Fig. 4). As previously reported (17), telomere-bound TRF1 was greatly reduced in cells expressing wild type TANK compared with TANK-PD-expressing cells (Fig. 4*A*). Similarly, the number and intensity of TIN2 foci decreased significantly in wild type TANK-expressing cells (Fig. 4*B*). The direct interaction between TIN2 and TRF2 suggests that TRF2 telomere localization may be affected in

TANK-expressing cells as well. Indeed, in cells in which TRF1 levels were reduced because of TANK expression, anti-TRF2 staining also decreased (Fig. 4*A*). Consistent with this observation, the amounts of chromatin-bound TIN2 and TRF2 in TANK-expressing cells were also reduced, as analyzed by Western blotting (Fig. 4*C*). These results are not only consistent with the finding that TRF2 telomere localization was altered in TRF1 knock-out cells (17) but also provide further support for the six-protein core telosome model. In this case, eliminating TRF1 could prevent telosome formation, thereby preventing telomere localization of TIN2 and TRF2. Therefore, telomere localization of TRF2 may depend upon the formation of telosome.

DISCUSSION

All six proteins, TRF1, TRF2, TIN2, RAP1, POT1, and PTOP, have been shown to specifically localize to the telomeres in mammalian cells. Functional interference with any of the six proteins by RNAi or dominant negative expression has been known to affect telomere length or end capping (3, 6–8, 12, 15, 23). Therefore, these proteins probably are the major players of telomere maintenance. In a recent study by Kim *et al.* (18), the authors showed a direct interaction between TIN2 and TRF2. In this report, we demonstrated that TIN2/TRF2 interaction provides only one piece of the puzzle, because all six telomeric proteins are able to assemble into a high molecular weight complex, the telosome. While this paper was in review, Ye *et al.* (27) also reported the discovery of the six-protein telomeric complex, which is consistent with our findings. The telosome model helps to explain why similar telomere extension phenotypes in human cells were obtained when RAP1, POT1, PTOP, or TIN2 was inhibited through RNAi or dominant negative expression (3, 6–8, 15, 23). Incorporation of the dominant negative forms of a subunit into the telosome may prevent its normal function, and knock-down of one of the six proteins by RNAi will probably hinder telosome formation. Additionally, the stoichiometry of telosome subunits may be crucial to its proper assembly. For example, the knock-down of TIN2 through RNAi led to reduced TRF1 localization at the telomeres (23). In further support of a critical role of the telosome in maintaining telomere integrity, inactivation of TIN2 or TRF1 in mice resulted in embryonic lethality (14, 30). In the TRF1 knock-out mouse, telomeric localization of TRF2 and TIN2 was also disrupted (17).

Both TRF1 and TRF2 can bind telomeric double-stranded DNA. The functional difference between these two proteins is probably due to their abilities to recruit different signaling complexes. TRF1 plays a primary role in telomere length control and cell cycle, whereas TRF2 protects telomere ends from being recognized as DNA breaks. It was unclear whether communication could occur between the TRF1 and TRF2 complexes. Our results suggested that TRF1 and TRF2 interact with each other through TIN2 and highlight the functional connection between TRF1 and TRF2. The identification of the telosome unites two essential pathways in telomere maintenance, telomere length, and end protection and suggests coordinated action and functional cross-talk between its subcomplexes. Functionally similar to the budding yeast telosome (28, 29), the mammalian telosome may represent the core telomere-associated complex mediating telomere maintenance in mammalian cells. Each of the six telomeric proteins may interact with many other different proteins to form unique subcomplexes, allowing for the dynamic integration and processing of signals from diverse pathways.

Acknowledgments—We thank Doug Chan and Amin Safari for technical assistance.

REFERENCES

1. de Lange, T. (2002) *Oncogene* **21,** 532–540
2. Kim Sh, S. H., Kaminker, P., and Campisi, J. (2002) *Oncogene* **21,** 503–511
3. van Steensel, B., and de Lange, T. (1997) *Nature* **385,** 740–743
4. Smith, S., and de Lange, T. (2000) *Curr. Biol.* **10,** 1299–1302
5. Smogorzewska, A., van Steensel, B., Bianchi, A., Oelmann, S., Schaefer, M. R., Schnapp, G., and de Lange, T. (2000) *Mol. Cell. Biol.* **20,** 1659–1668
6. Loayza, D., and De Lange, T. (2003) *Nature* **424,** 1013–1018
7. Liu, D., Safari, A., O'Connor, M. S., Chan, D. W., Laegeler, A., Qin, J., and Songyang, Z. (2004) *Nat. Cell Biol.* **6,** 673–680
8. Ye, J. Z., Hockemeyer, D., Krutchinsky, A. N., Loayza, D., Hooper, S. M., Chait, B. T., and de Lange, T. (2004) *Genes Dev.* **18,** 1649–1654
9. Zhou, X. Z., and Lu, K. P. (2001) *Cell* **107,** 347–359
10. Griffith, J. D., Comeau, L., Rosenfield, S., Stansel, R. M., Bianchi, A., Moss, H., and de Lange, T. (1999) *Cell* **97,** 503–514
11. Wei, C., and Price, M. (2003) *Cell Mol. Life Sci.* **60,** 2283–2294
12. van Steensel, B., Smogorzewska, A., and de Lange, T. (1998) *Cell* **92,** 401–413
13. Zhu, X. D., Kuster, B., Mann, M., Petrini, J. H., and de Lange, T. (2000) *Nat. Genet.* **25,** 347–352
14. Zhu, X. D., Niedernhofer, L., Kuster, B., Mann, M., Hoeijmakers, J. H., and de Lange, T. (2003) *Mol. Cell* **12,** 1489–1498
15. O'Connor, M. S., Safari, A., Liu, D., Qin, J., and Songyang, Z. (2004) *J. Biol. Chem.* **279,** 28585–28591
16. Karlseder, J., Smogorzewska, A., and de Lange, T. (2002) *Science* **295,** 2446–2449
17. Iwano, T., Tachibana, M., Reth, M., and Shinkai, Y. (2003) *J. Biol. Chem.* **279,** 1442–1448
18. Kim, S. H., Beausejour, C., Davalos, A. R., Kaminker, P., Heo, S. J., and Campisi, J. (2004) *J. Biol. Chem.* **279,** 43799–43804
19. Kim, S. H., Kaminker, P., and Campisi, J. (1999) *Nat. Genet.* **23,** 405–412
20. Li, B., Oestreich, S., and de Lange, T. (2000) *Cell* **101,** 471–483
21. Baumann, P., and Cech, T. R. (2001) *Science* **292,** 1171–1175
22. Colgin, L. M., Baran, K., Baumann, P., Cech, T. R., and Reddel, R. R. (2003) *Curr. Biol.* **13,** 942–946
23. Ye, J. Z., and de Lange, T. (2004) *Nat. Genet.* **36,** 618–623
24. Ogryzko, V. V., Kotani, T., Zhang, X., Schiltz, R. L., Howard, T., Yang, X. J., Howard, B. H., Qin, J., and Nakatani, Y. (1998) *Cell* **94,** 35–44
25. Smith, S., Giriat, I., Schmitt, A., and de Lange, T. (1998) *Science* **282,** 1484–1487
26. Chang, W., Dynek, J. N., and Smith, S. (2003) *Genes Dev.* **17,** 1328–1333
27. Ye, J. Z., Donigian, J. R., Van Overbeek, M., Loayza, D., Luo, Y., Krutchinsky, A. N., Chait, B. T., and De Lange, T. (2004) *J. Biol. Chem.* **279,** 47264–47271
28. Wright, J. H., Gottschling, D. E., and Zakian, V. A. (1992) *Genes Dev.* **6,** 197–210
29. Dubrana, K., Perrod, S., and Gasser, S. M. (2001) *Curr. Opin. Cell Biol.* **13,** 281–289
30. Chiang, Y. J., Kim, S., Tessarollo, L., Campisi, J., and Hodes, R. J. (2004) *Mol. Cell. Biol.* **24,** 6631–6634